

# Supplementary Information

## Unexpected triaxial preferences in some all-*syn* 1,3,5-trifluorocyclohexanes

Cihang Yu,<sup>a</sup> Bruno A. Piscelli,<sup>b</sup> Nawaf Al Maharik,<sup>c</sup> David B. Cordes,<sup>a</sup> Alexandra M. S. Slawin,<sup>a</sup> Rodrigo A. Cormanich,<sup>\*b</sup> David O'Hagan<sup>\*a</sup>

### Index:

Material and methods	Page 2
Images of NMR Spectra	Page 8
Details of X-Ray Diffractions data	Page 23
Details of Computational Calculations	Page 26

# Material and Methods

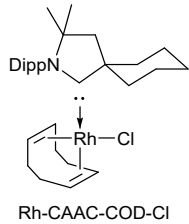
All reactions were carried out under argon atmosphere with standard Schlenk techniques unless otherwise specified. The reaction glassware were oven dried and cooled under vacuum. Commercially available chemicals were purchased from Acros, Alfa Aeser, Fisher Scientific, Fluorochem, Sigma Aldrich, Strem Chemicals, and TCI (UK) and used as received unless otherwise stated. Anhydrous solvent such as DCM, diethyl ether, THF, toluene and hexane were dried in solvent purification system (Mbraun MB SPS-200).

The hydrogenation reactions were performed in a steel high pressure autoclave at the indicated pressure and temperature. The reaction mixture was loaded onto a dry microwave or glass vessel tube equipped with a cross magnetic stirring bar and transferred to the Autoclave under argon. *In vacuo* refer to the use of rotary evaporator with membrane pump to 30-50 mbar at 40 °C unless otherwise stated.

<sup>1</sup>H, <sup>13</sup>C and <sup>19</sup>F NMR spectra were recorded on Bruker AVIII-HD 700 Hz with Cryo Probe Prodigy TCI (<sup>1</sup>H, 700 MHz, <sup>13</sup>C, 176 MHz, <sup>19</sup>F, 659 MHz), Bruker AVIII 500 Hz with Cyro Probe Prodigy BBO or Bruker AVIII-HD 500 Hz with SmartProbe BBFO+ (500 MHz <sup>1</sup>H, 125 MHz <sup>13</sup>C, and 470 MHz for <sup>19</sup>F) or Bruker AV 400 Hz with BBFO probe (400 MHz <sup>1</sup>H, 100 MHz <sup>13</sup>C, 161 MHz and 376 MHz for <sup>19</sup>F). NMR analyses were carried out at room temperature in indicated deuterated solvents unless otherwise noted. Chemical shifts data were reported as δ units of ppm corrected by solvent residue peak and coupling constants, J, are reported in Hz. Multiplicities are indicated by: s for singlet, d for doublet, t for triplet, q for quartet and m for multiplet and br. for broad brand. Analytical thin layer chromatography was carried out on aluminium backed Merck TLC silica gel 60 F<sub>254</sub> plates. These plates were visualised using UV light at 254 nm wavelength, dyed by potassium permanganate or phosphomolybdic acid followed by heating. Flash column chromatography performed with Sigma-Aldrich silica gel, 60 Å pore size and 230-400 mesh, 40-63 μm particle size under 5-10 psi compressed air. Melting points were measured on a Griffin electric thermal melting point apparatus with thermometer and reading are uncorrected. Mass spectra measurements were carried by University of St Andrews Mass Spectrometer Facility using ESI.

## Catalyst synthesis

The preparation of Rh(CAAC)(COD)Cl following the reported literature<sup>1</sup> with modification. Commercially available ligand (CAAC)<sup>·</sup>2HCl was used instead of synthetic carbene salt (CAAC)HCl therefore an additional equivalent of base was added.

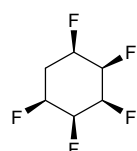


[Rh(COD)Cl]<sub>2</sub> precursor (161 mg, 0.326 mmol, 0.5 eq.), carbene salt of CAAC·2HCl and KHMDS was added to a Schlenk tube in glove box under nitrogen atmosphere, Dry THF (15 ml) were added dropwise over 10 min to the vigorous stirring solid/suspension mixture. The suspension was stirred for another 10 min at -78, after which the cooling dry ice/acetone bath is removed. After stirring for 16 h at r.t., the reaction mixture is filtered, the residue was washed with THF (10 ml), concentrated and dried under high vacuum. The product was dissolved in diethyl ether, adsorbed onto silica gel and purified by column chromatography (pentane: diethyl ether 19:1). After evaporation of the solvent, the complex was titurated from a concentrated DCM solution with pentane to yield desired complex as yellow powder. Yield 55 %. <sup>1</sup>H NMR (400 MHz, CDCl<sub>3</sub>): δ = 7.45–7.37 (m, 2H), 7.14 (dd, *J* = 1.6, 6.4 Hz, 1H), 5.24 (t, *J* = 7.2 Hz, 1H), 4.60 (q, *J* = 8.0 Hz, 1H), 3.92–3.86 (m, 1H), 3.45–3.43 (m, 1H), 2.92–2.84 (m, 2H), 2.63–2.45 (m, 3H), 2.28–2.25 (m, 1H), 2.14–2.11 (m, 1H), 2.01–1.92 (m, 3H), 1.78–1.73 (m, 7H), 1.58–1.55 (m, 2H), 1.49 (s, 3H), 1.44–1.35 (m, 3H), 1.26–1.22 (m, 9H), 1.19 (s, 3H), 0.94 (d, *J* = 6.8 Hz, 3H). The <sup>1</sup>H NMR match to literature value<sup>1</sup>.

## General reaction conditions for arene hydrogenation

Fluoroarene substrate (1 mmol), oven dried silica/ 4Å MS (1g), Rhodium CAAC catalyst (1 mmol %) and dry hexane (10ml) were added under argon to a 100 ml glass tube vessel. The reaction vessel was placed in a 150 ml stainless steel autoclave. The autoclave was pressurised and de-pressurised with 5 bar hydrogen three times before being charged to 50 bar of hydrogen. The reaction mixture was stirred at room temperature for 24 h, after which the autoclave was de-pressurised. The reaction mixture was flushed with DCM, acetone or methanol onto silica, dried and submitted to column chromatography.

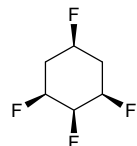
### All-*cis*-1,2,3,4,5-pentafluorocyclohexane (**3**)



Product **3** was prepared by the standard hydrogenation method. The crude product was directly submitted to column chromatography with DCM to generate **3** as a white solid (39 % yield). M.p. 150–152 °C

<sup>1</sup>H NMR (318 K, 500 MHz, Methanol-*d*<sub>4</sub>) δ 5.05 (dt, *J* = 51.5, 11.9 Hz, 1H), 4.86 – 4.67 (m, 1H), 2.49 (h, *J* = 10.2 Hz, 1H), 2.33 – 2.20 (m, 1H). <sup>19</sup>F NMR (213 K, 470 MHz, Methanol-*d*<sub>4</sub>) δ -200.9 – -201.1 (m), -213.2 (t, *J* = 12.0 Hz), -219.32 (ddd, *J* = 12.0, 7.1, 4.8 Hz). Data matched the literature<sup>1</sup>.

#### All-*cis*-1,2,3,5-tetrafluorocyclohexane (**4**)

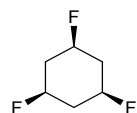


Product **4** was prepared by the standard hydrogenation method. The crude product was directly submitted to column chromatography (DCM/Pentane). A white solid (65% yield) was recovered after concentrated *in vacuo*. M.p. 84–86 °C.

<sup>1</sup>H NMR (500 MHz, Chloroform-*d*) δ 5.06 (dtd, *J* = 54.3, 10.4, 2.1 Hz, 1H), 4.71 – 4.22 (m, 3H), 2.44 (dt, *J* = 11.9, 6.0 Hz, 2H), 2.35 – 2.09 (m, 2H). <sup>19</sup>F NMR (471 MHz, Chloroform-*d*) δ -183.9 (dd, *J* = 46.7, 8.8 Hz), -197.0 (ddd, *J* = 44.9, 15.6, 8.2 Hz), -216.1 – -218.2 (m). <sup>13</sup>C NMR (126 MHz, Chloroform-*d*) δ 87.53 (dt, *J* = 188.0, 17.9 Hz), 86.20 – 82.84 (m, overlapped), 32.10 (td, *J* = 21.4, 3.9 Hz).

Mass FTMS +P ESI [M+Na] observed 179.0453 calculated as 179.0455.

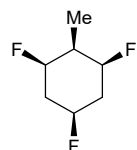
#### All-*cis*-1,3,5-trifluorocyclohexane (**5**)



Product **5** was prepared by the standard hydrogenation method. The crude product was directly submitted to a column chromatography (DCM/Pentane) and the product was recovered in 60 % yield as a white solid. M.p. 90 °C.

<sup>1</sup>H NMR (500 MHz, Methylene Chloride-*d*<sub>2</sub>) δ 4.58 (dtt, *J* = 45.8, 8.5, 3.7 Hz, 3H), 2.56 – 2.23 (m, 3H), 1.89 (h, *J* = 11.1 Hz, 3H). <sup>19</sup>F NMR (471 MHz, Methylene Chloride-*d*<sub>2</sub>) δ -181.4 (dp, *J* = 48.2, 12.6 Hz). <sup>13</sup>C NMR (126 MHz, Chloroform-*d*) δ 85.1 (dt, *J* = 176.0, 14.9 Hz), 37.8 (t, *J* = 20.0 Hz). All spectra and m.p match to the literature<sup>1</sup>.

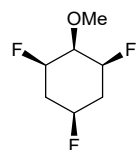
**(1*R*,2*s*,3*S*,5*r*)-1,3,5-Trifluoro-2-(trifluoromethyl) cyclohexane (6)**



Product **6** was prepared by the standard hydrogenation method. The crude product was directly submitted to column chromatography with DCM/Pentane. Yield 88%. M.p.88-90 °C

<sup>1</sup>H NMR (500 MHz, Chloroform-*d*) δ 4.68 (dddt, *J* = 50.1, 46.3, 7.3, 3.2 Hz, 3H), 2.47 – 2.28 (m, 2H), 2.24 – 1.91 (m, 3H), 1.20 (d, *J* = 7.1 Hz, 3H). <sup>19</sup>F NMR (470 MHz, CDCl<sub>3</sub>) δ -179.2, -192.0. <sup>13</sup>C NMR (126 MHz, Chloroform-*d*) δ 88.2 (d, *J* = 180.6 Hz), 84.9 (d, *J* = 175.3 Hz), 37.5 (t, *J* = 19.6 Hz), 34.8 – 33.3 (m), 10.1. FTMS + P ESI observed [M+Na] 175.0703, calculated 175.0711

**(1*R*,2*s*,3*S*,5*r*)-1,3,5-Trifluoro-2-methoxycyclohexane (7)**

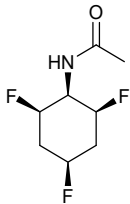


Product **10** was prepared by the standard hydrogenation method. The crude product is directly submitted to column chromatography with DCM/Pentane. The product was isolated as a colourless oil (Yield 47 %). The compound was cooled to -20 °C in a freezer for crystallisation.

<sup>1</sup>H NMR (500 MHz, Acetone-*d*<sub>6</sub>) δ 4.83 – 4.49 (m, 3H), 3.96 (td, *J* = 9.6, 2.5 Hz, 1H), 3.54 (s, 3H), 2.31-2.23 (m, 2H), 2.16 – 2.01 (m, 2H). <sup>19</sup>F NMR (470 MHz, Acetone) δ -183.1, -195.7.

<sup>13</sup>C NMR (126 MHz, Acetone-*d*<sub>6</sub>) δ 88.2 (ddd, *J* = 181.4, 17.1, 13.0 Hz), 85.6 (dt, *J* = 173.4, 18.0 Hz), 78.9 (t, *J* = 17.0 Hz), 60.7, 55.1, 33.2 (t, *J* = 21.0 Hz). FTMS + P ESI observed [M+Na] 191.0652, calculated 191.0660

**N-((1s,2R,4r,6S)-2,4,6-trifluorocyclohexyl) acetamide (9)**

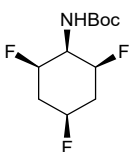


Product **9** was prepared by the standard hydrogenation method using 2 mmol % of catalyst, hexane (14 ml) and silica (1 g) per 1 mmol substrate. The reaction time was extended to 3 days. The compound was purified over silica gel (acetone/DCM) and recrystallized in hot toluene to afford colourless needles (18 % yield. M.p. 126–130 °C).

<sup>1</sup>H NMR (700 MHz, Toluene-*d*<sub>8</sub>) δ 4.36 (overlapped, br, 2H), 4.16 (d, *J* = 47.7 Hz, 1H), 3.90 – 3.54 (m, 2H), 1.74 (d, *J* = 11.5 Hz, 3H), 1.12 (m, 2H), 0.77 (m, 2H).

<sup>19</sup>F NMR (659 MHz, Toluene-*d*<sub>8</sub>) δ -179.8, -196.2. <sup>13</sup>C NMR (176 MHz, Tol) δ 88.3, 89.2, 84.9, 85.7, 47.8, 33.0, 24.94, 33.0 FTMS + P ESI Calculated ESI[M+Na] 218.0763 observed 218.0755.

**tert-Butyl ((1s,2R,4r,6S)-2,4,6-trifluorocyclohexyl) carbamate (10)**

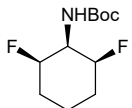


Aryl hydrogenation to generate **10** was carried out with 4 Å MS and a hydrogenation for 3 days. The product was purified over silica gel (acetone/DCM) and dried *in vacuo* to afford a white fibrous solid (40% yield, M.p. 160–162 °C (sub.)).

<sup>1</sup>H NMR (500 MHz, Acetone-*d*<sub>6</sub>) δ 6.08 (s, 1H), 4.85 (ddt, *J* = 44.0, 23.8, 4.3 Hz, 4H), 4.05 (tdt, *J* = 26.5, 9.7, 3.3 Hz, 1H), 2.50 – 2.39 (m, 2H), 2.29 – 2.10 (m, 3H), 1.44 (s, 9H, <sup>1</sup>Bu). <sup>19</sup>F NMR (470 MHz, Acetone-*d*<sub>6</sub>) δ -178.5, 1F, -195.3. <sup>13</sup>C NMR (126 MHz, Acetone-*d*<sub>6</sub>) δ 88.2 (d, *J* = 180.6 Hz), 85.3 (dt, *J* = 174.0, 4.4 Hz), 79.6, 52.2 (t, *J* = 17.6 Hz), 34.4 (ddd, *J* = 20.3, 13.0, 7.0 Hz), 28.6.

FTMS + P ESI observed [M+Na] 276.1179, calculated 276.1187.

**tert-Butyl ((1*s*,2*R*,6*S*)-2,6-difluorocyclohexyl) carbamate (12)**



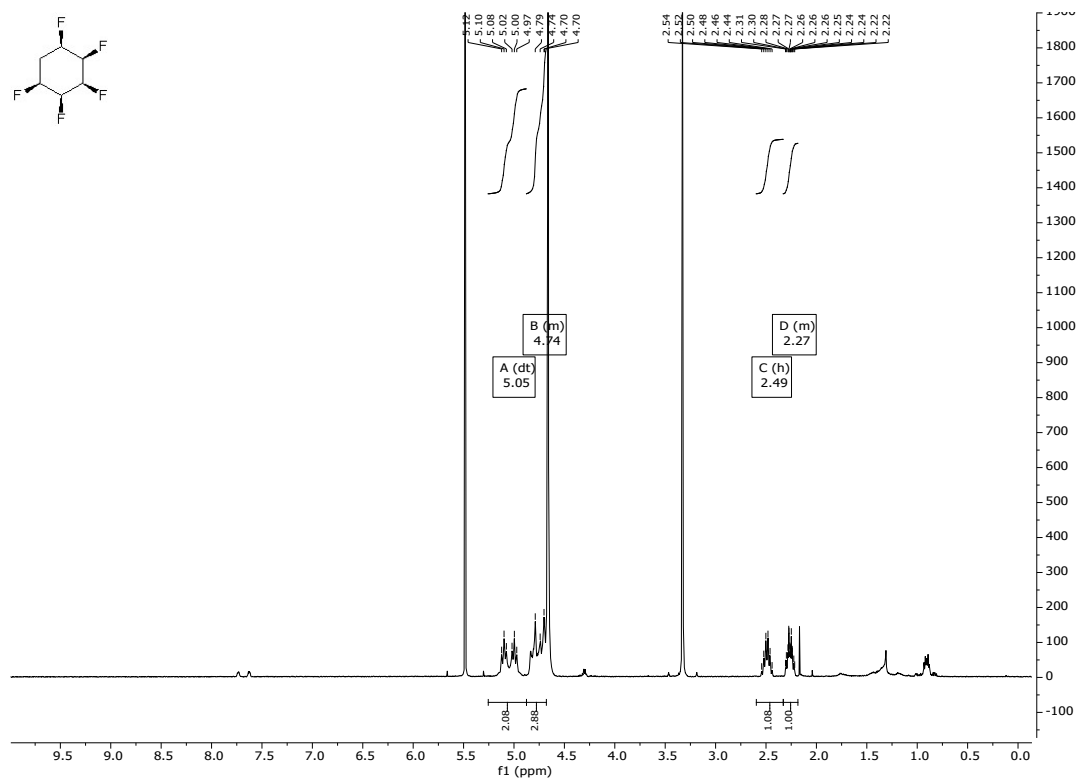
Rhodium catalyst (7 mg), tert-butyl (2,6-difluorophenyl) carbamate (0.2 g, 1 mmol) and activated 4 Å MS (250 mg) in a hexane (15 mL) solution were stirred under a hydrogen atmosphere under reduced pressure at 40 °C for 2 days. The product was purified by column chromatography (pentane/dichloromethane 1:1 to dichloromethane/acetone 98:2) to give **12** (73 mg, 31% yield) as a white solid; m.p. = 92-93 °C;

<sup>1</sup>H NMR (400 MHz, Chloroform-*d*) δ 5.37 (d, *J* = 9.1 Hz, 1H, NH), 4.79 (d, *J* = 47.2 Hz, 2H, CHF), 3.66 (td, *J* = 33.2, 9.7 Hz, 1H, CHN), 2.28 – 2.09 (m, 2H,), 1.88 (qt, *J* = 13.5, 3.9 Hz, 1H), 1.65 – 1.48 (m, 2H), 1.45 (9H, s) 1.44 (d, *J*=12.1 Hz). <sup>19</sup>F NMR (376 MHz, Chloroform-*d*) δ -198.1. <sup>13</sup>C NMR (101 MHz, CDCl<sub>3</sub>) δ 155.5, 90.4 (d, *J*=174.7 Hz), 80.2, 52.0 (t, *J* = 17.0 Hz), 29.8 (dd, *J* = 12.6, 8.3 Hz), 28.5, 13.2. HRMS (EI, +ve) m/z calculated for C<sub>11</sub>H<sub>19</sub>NO<sub>2</sub>F<sub>2</sub>Na [M+Na]<sup>+</sup> 258.1282, found 258.1272.

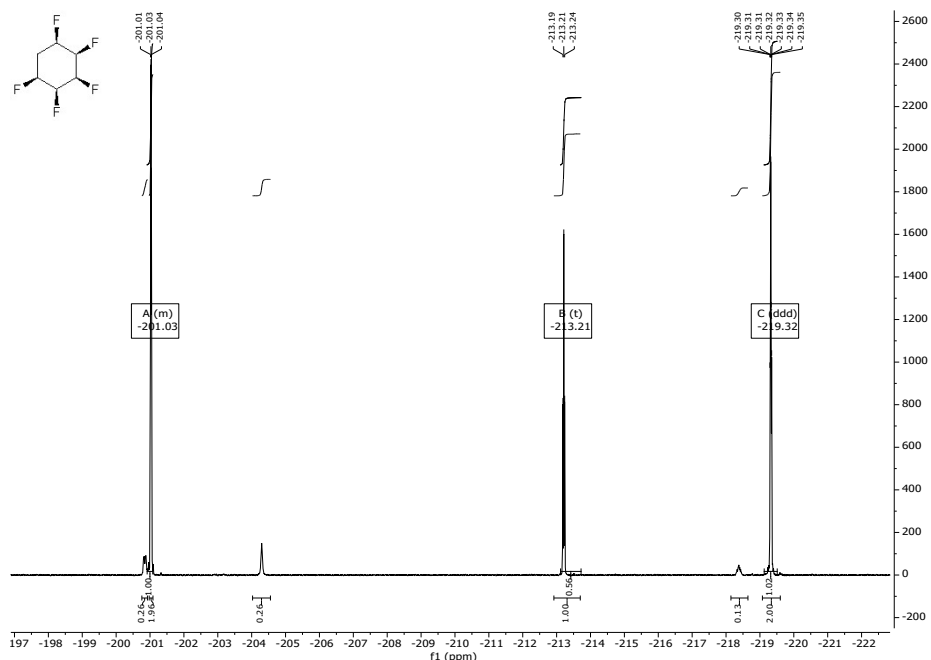
# Images of NMR Spectra

## all-*cis*-1,2,3,4,5-pentafluorocyclohexane (3)

$^1\text{H}$  NMR (500 MHz, Methanol- $d_4$ )

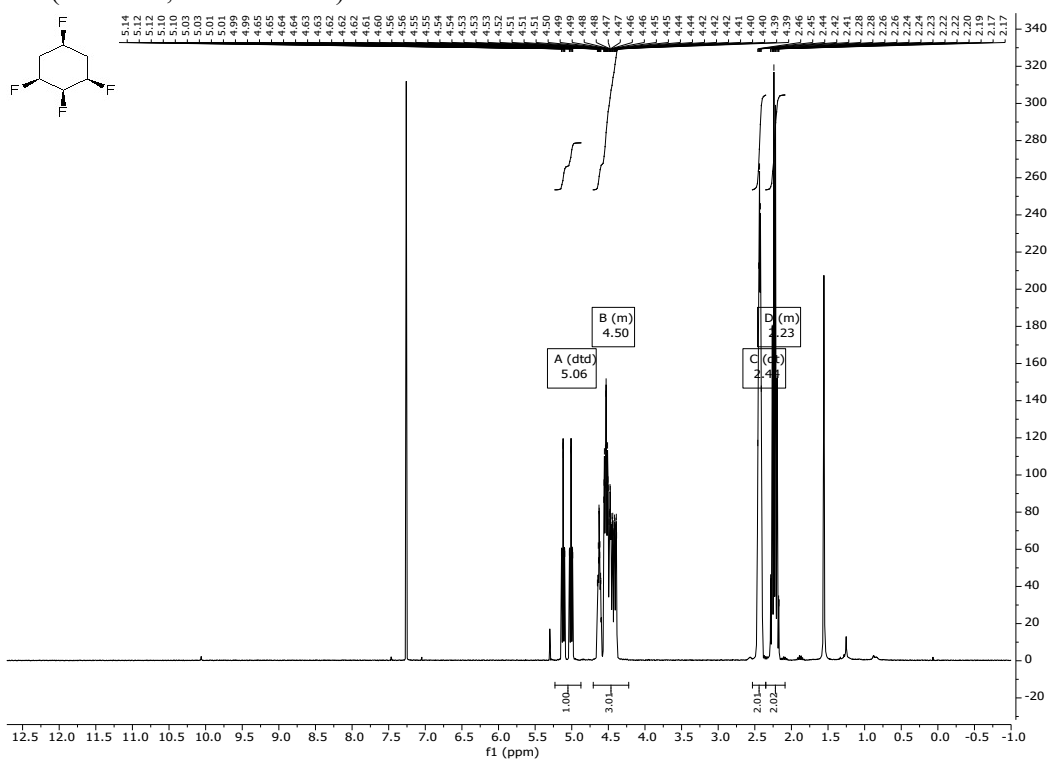


$^{19}\text{F}$  NMR (470 MHz, Methanol- $d_4$ )

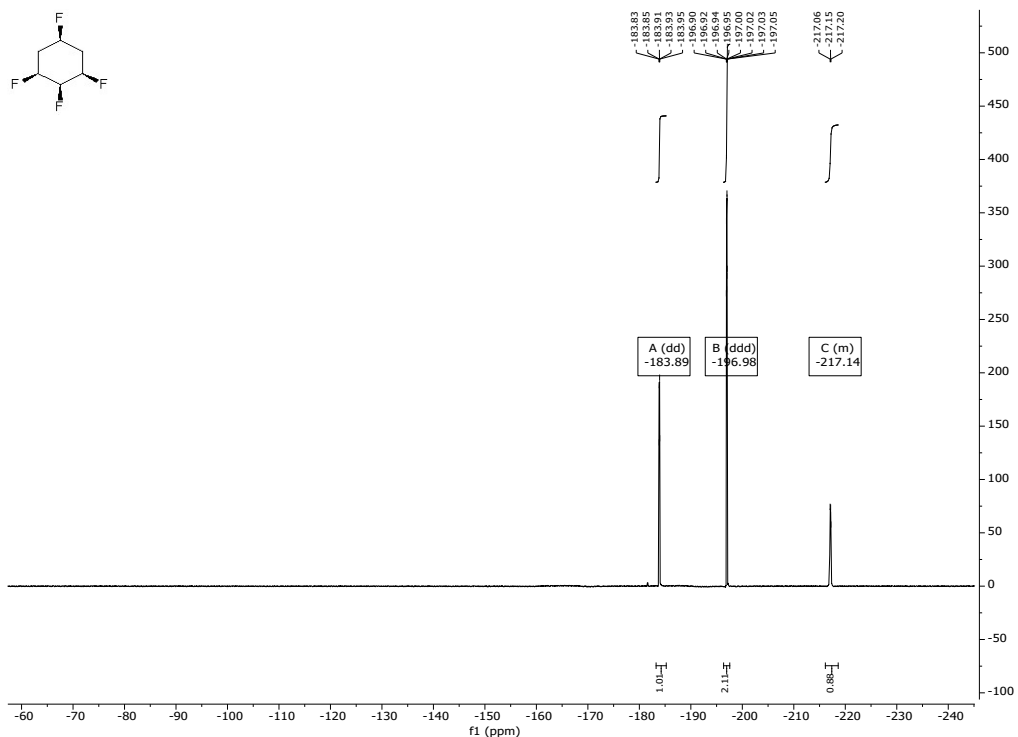


**all-*cis*-1,2,3,5-tetrafluorocyclohexane (4)**

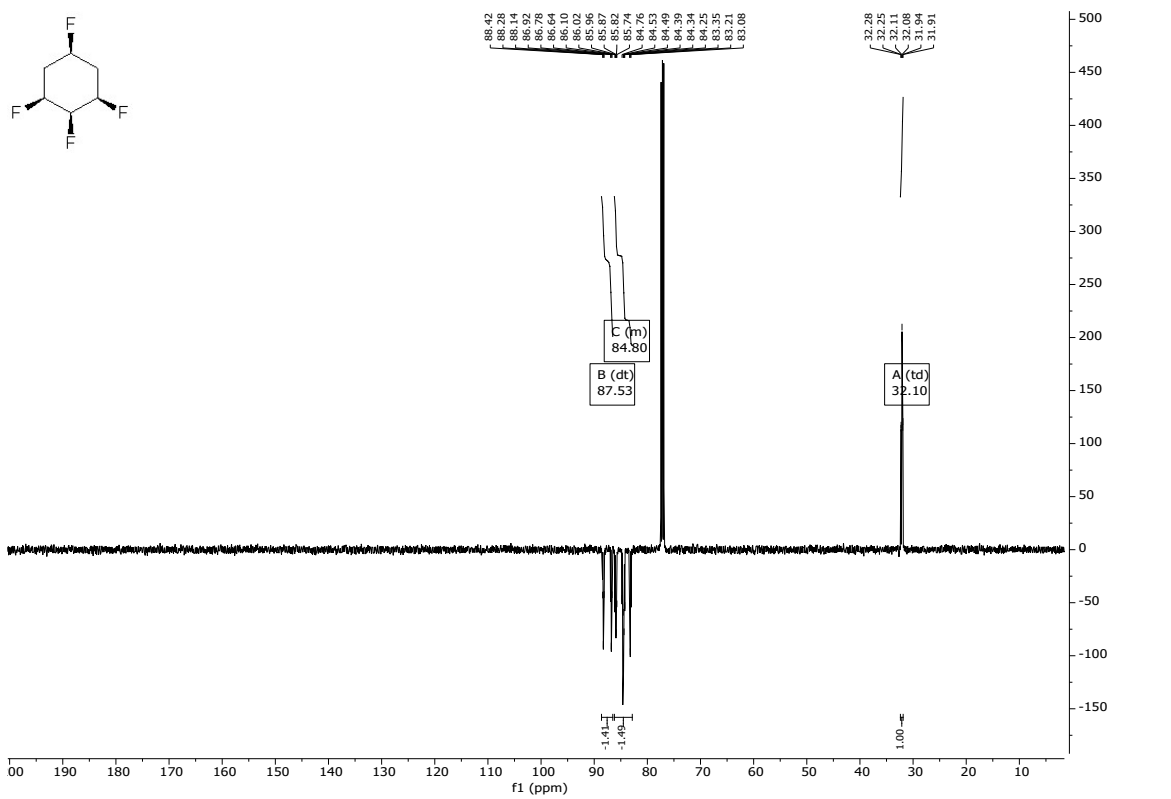
<sup>1</sup>H NMR (500 MHz, Chloroform-*d*)



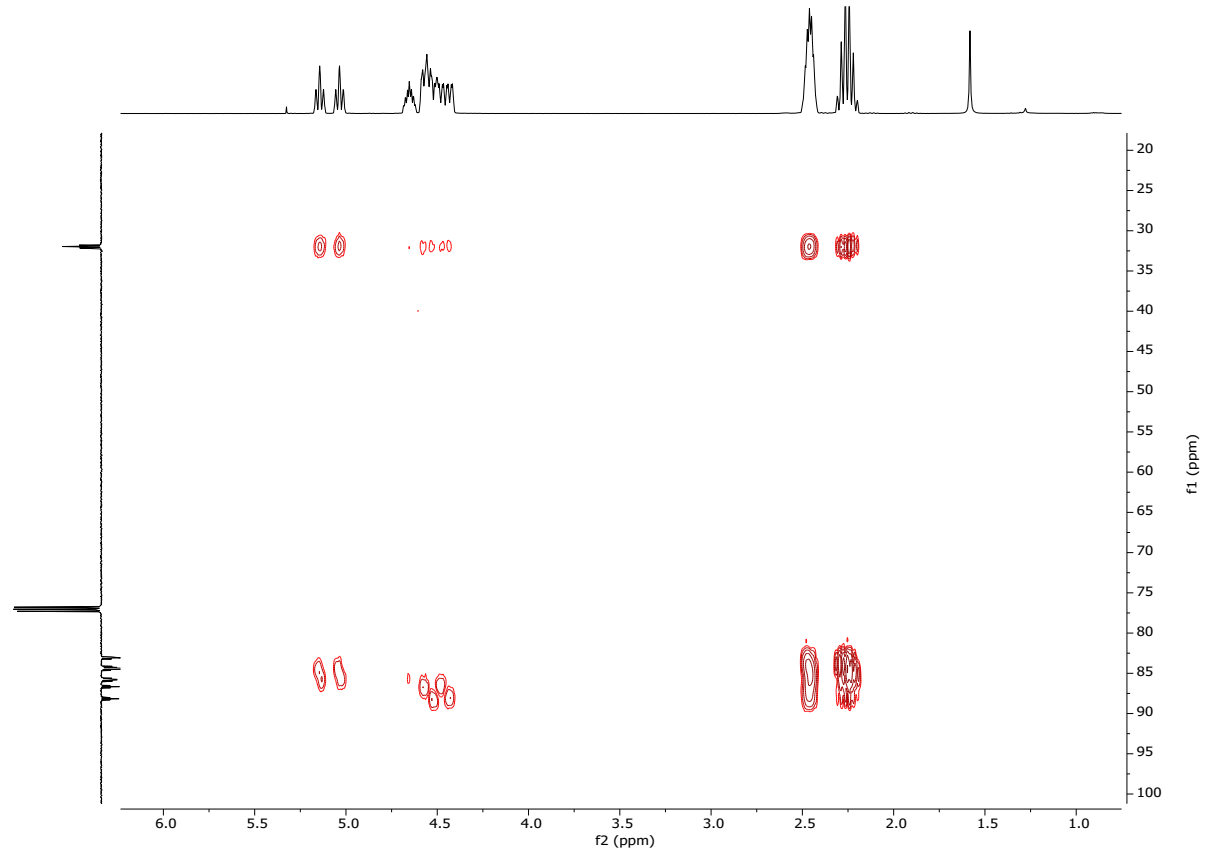
<sup>19</sup>F NMR (471 MHz, Chloroform-*d*)



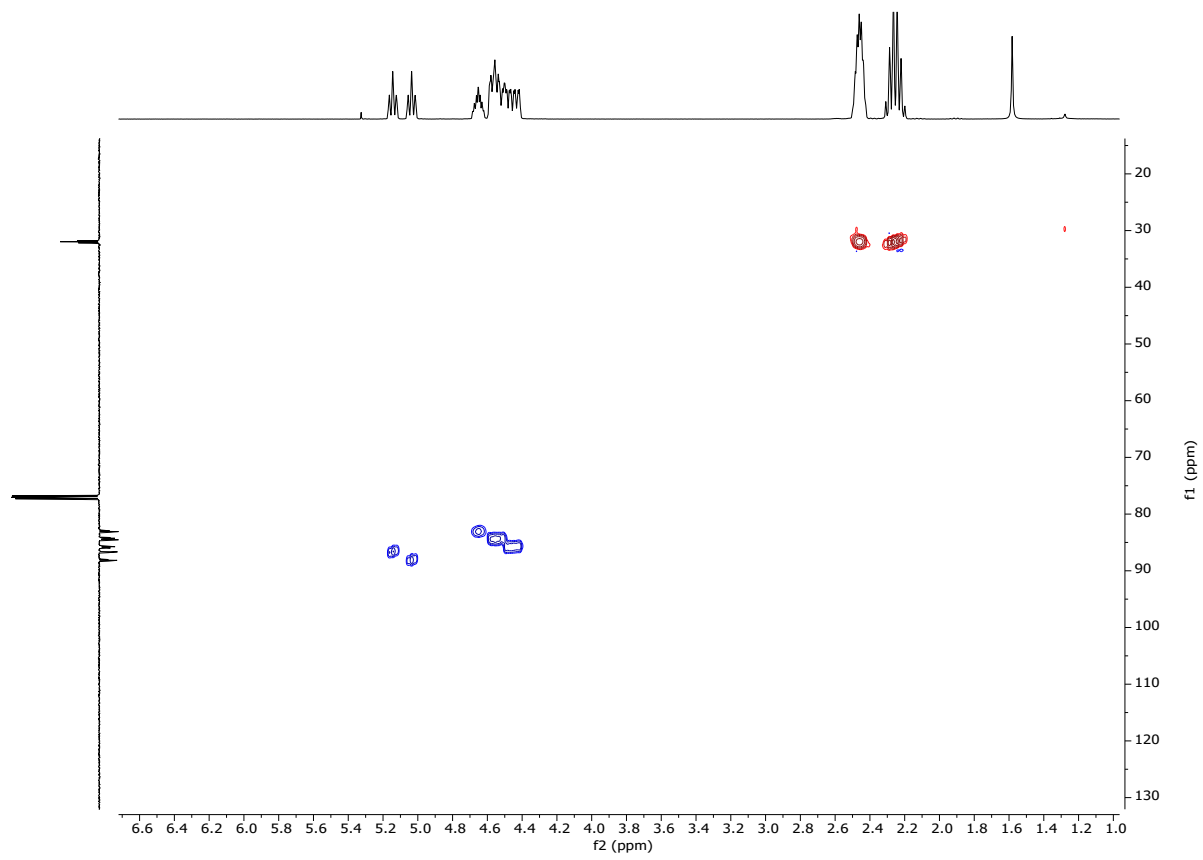
<sup>13</sup>C NMR (126 MHz, Chloroform-*d*)



2D <sup>1</sup>H, <sup>13</sup>C-gs-HMBC, CDCl<sub>3</sub>

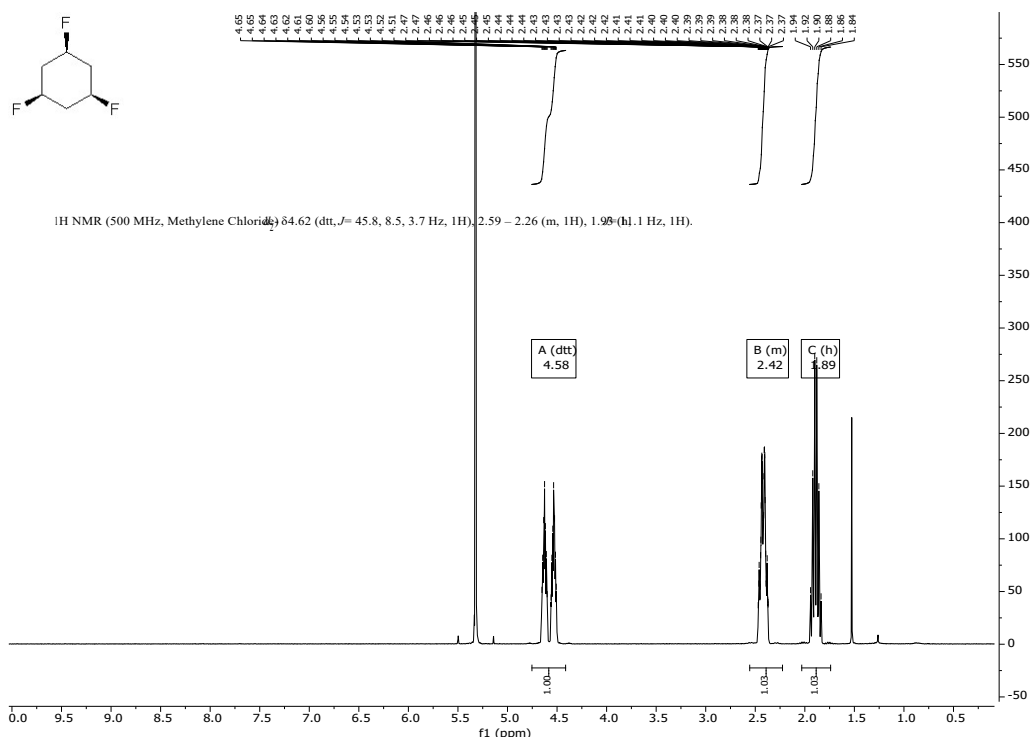


2D <sup>1</sup>H, <sup>13</sup>C-gs-HSQC with multiplicity editing

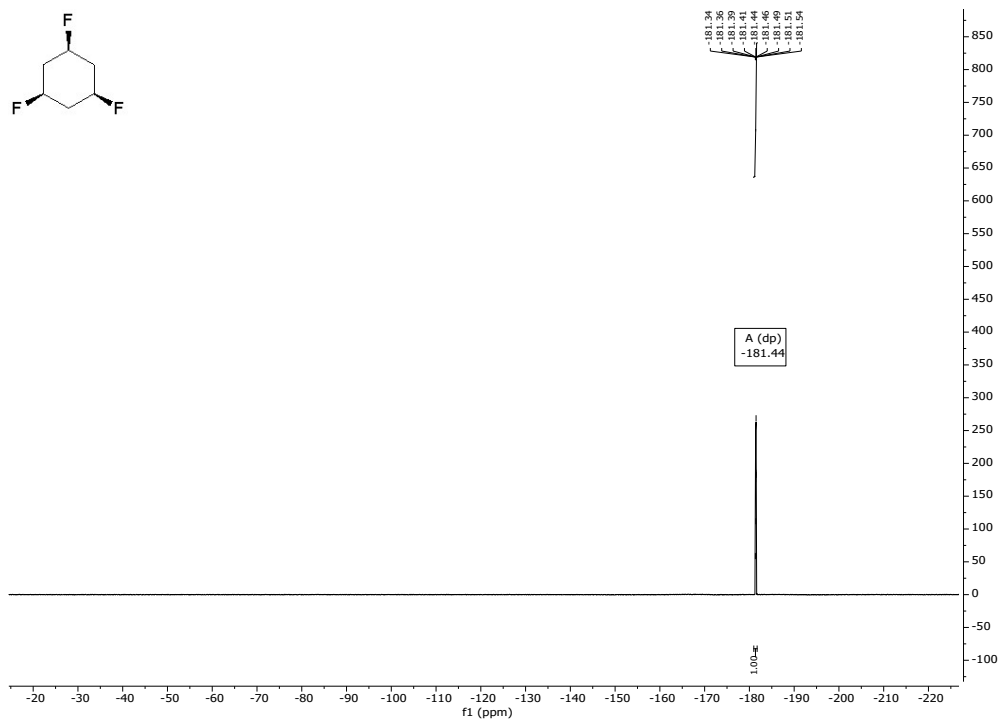


**all-*cis*-1,3,5-trifluorocyclohexane (5)**

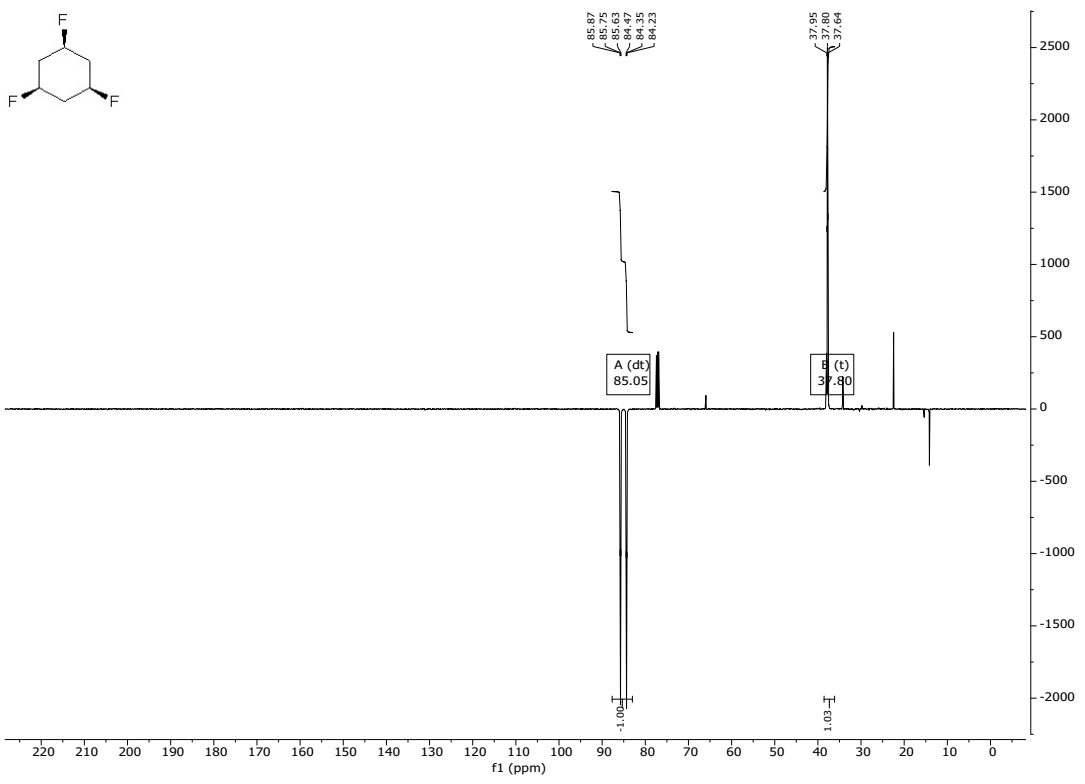
<sup>1</sup>H NMR (500 MHz, Methylene Chloride-*d*<sub>2</sub>)



<sup>19</sup>F NMR (471 MHz, Methylene Chloride-*d*<sub>2</sub>)

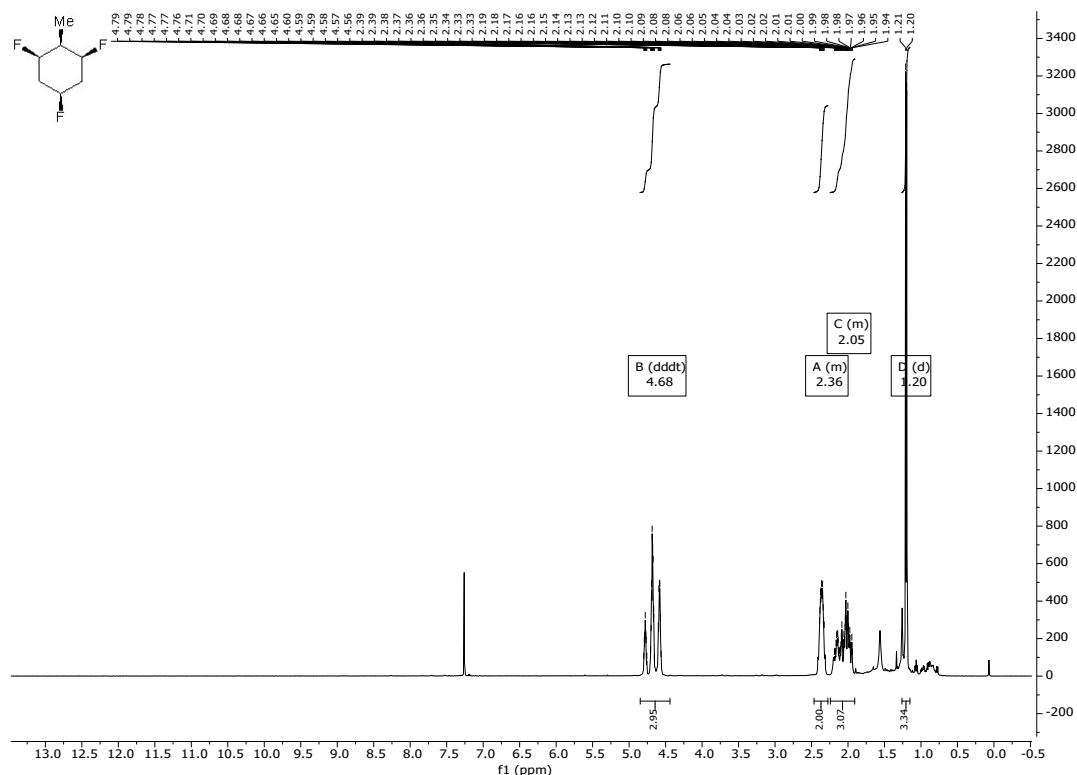


<sup>13</sup>C NMR (126 MHz, Chloroform-*d*)

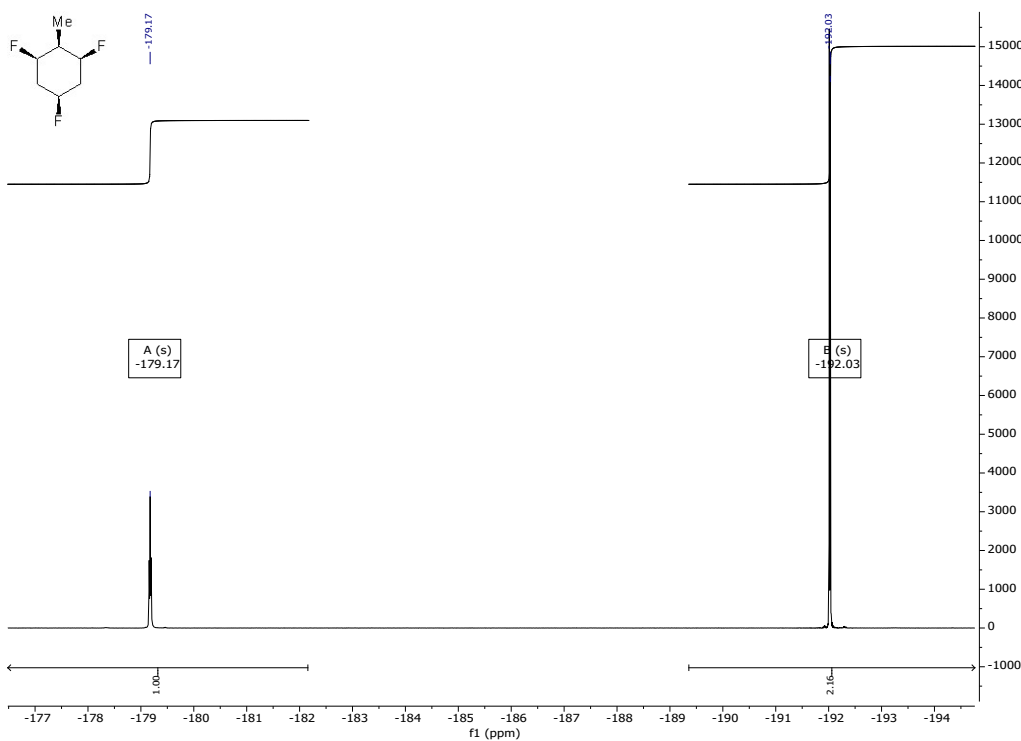


**(1*R*,2*s*,3*S*,5*r*)-1,3,5-trifluoro-2-(trifluoromethyl) cyclohexane (**6**)**

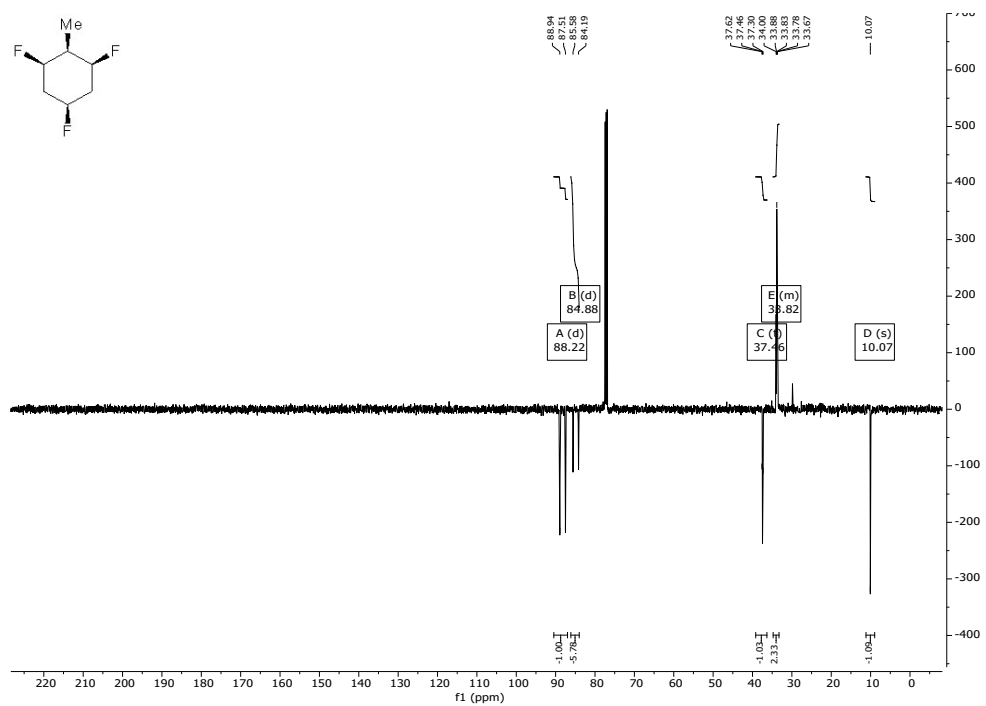
<sup>1</sup>H NMR (500 MHz, Chloroform-*d*)



<sup>19</sup>F NMR (470 MHz, *CDCl*<sub>3</sub>)

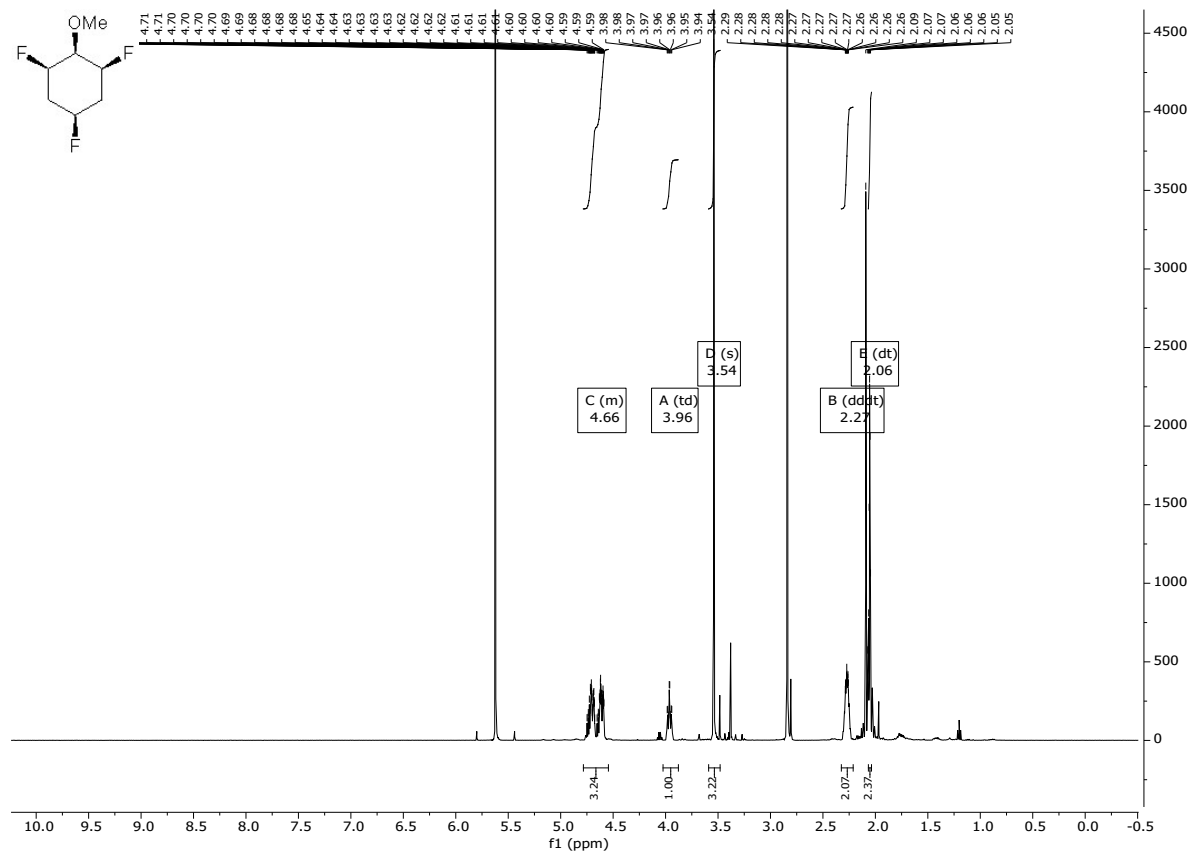


<sup>13</sup>C NMR (126 MHz, Chloroform-d)

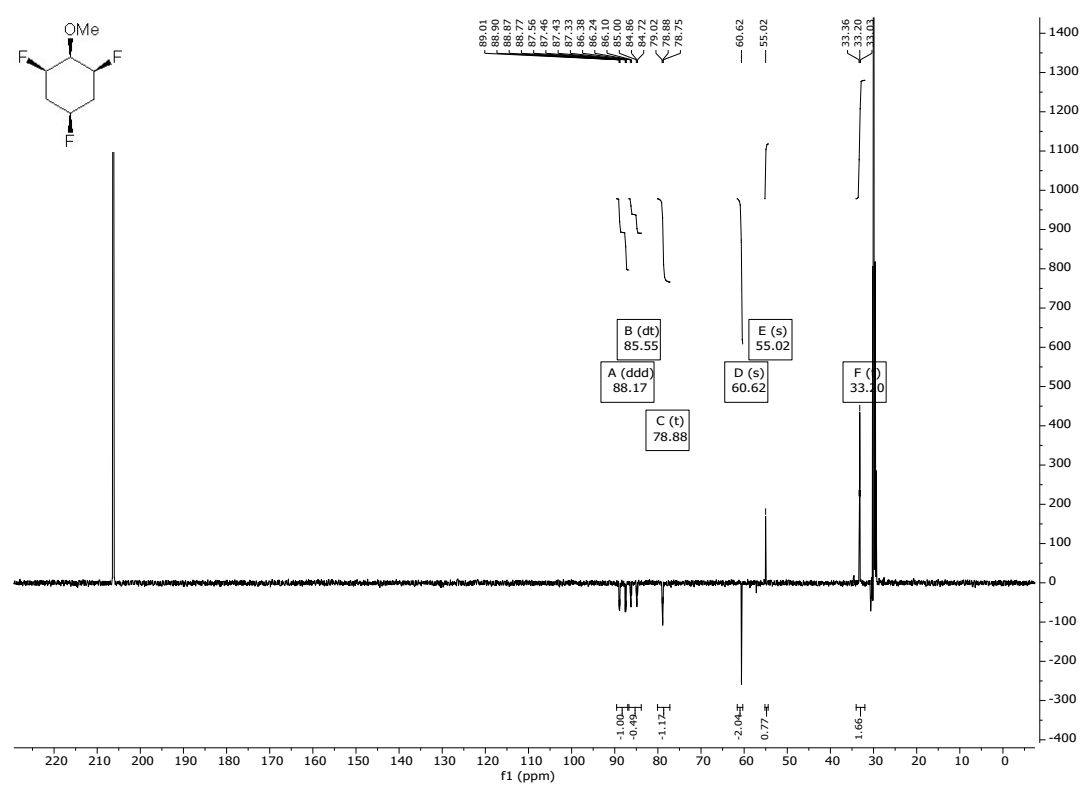
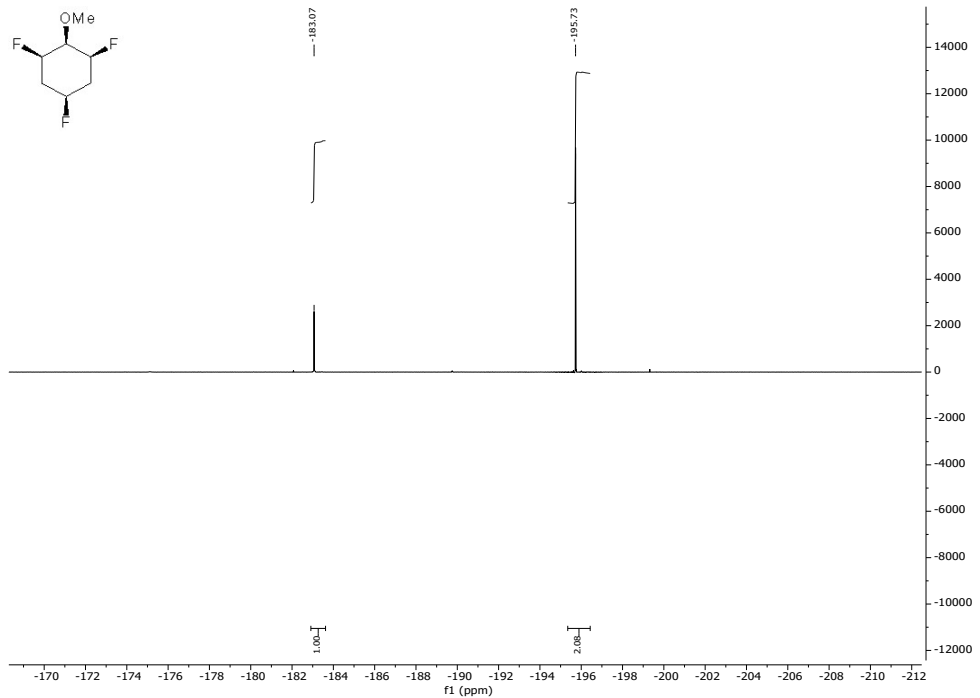


**(1*R*,2*s*,3*S*,5*r*)-1,3,5-trifluoro-2-methoxycyclohexane (7)**

<sup>1</sup>H NMR (500 MHz, Acetone-*d*<sub>6</sub>)

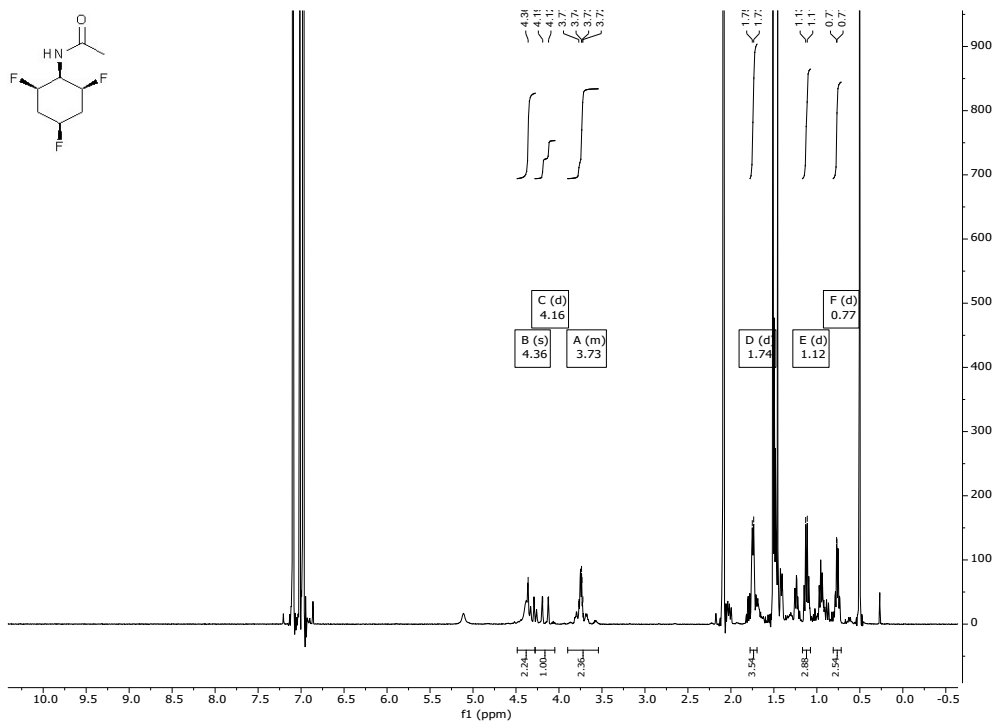


<sup>19</sup>F NMR (470 MHz, Acetone)

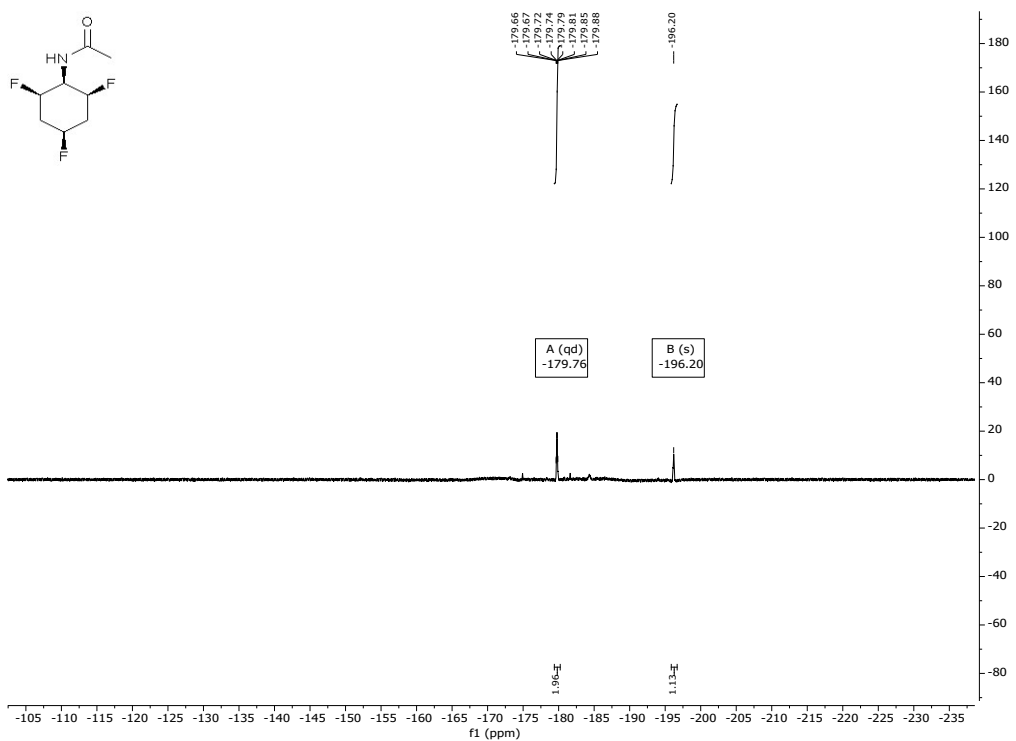


***N*-((1*s*,2*R*,4*r*,6*S*)-2,4,6-trifluorocyclohexyl) acetamide (9)**

<sup>1</sup>H NMR (700 MHz, Toluene-*d*<sub>8</sub>)

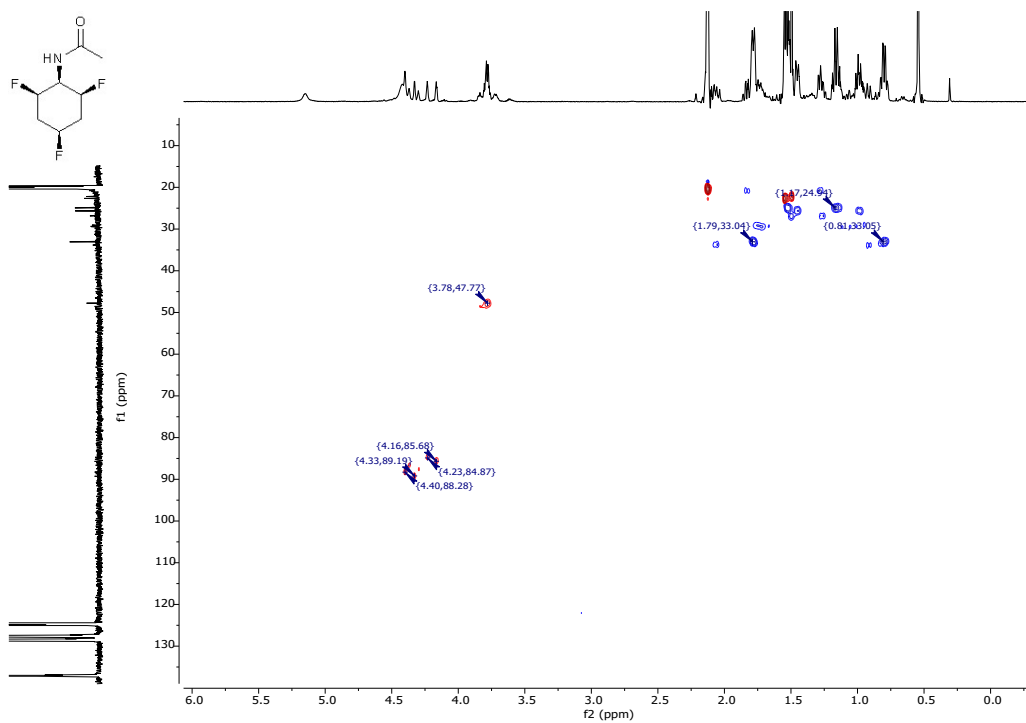


<sup>19</sup>F NMR (659 MHz, Toluene-*d*<sub>8</sub>) δ -179.77 (qd, *J* = 44.6 Hz, 13.3 Hz, 2F), -196.20 (s, 1F).



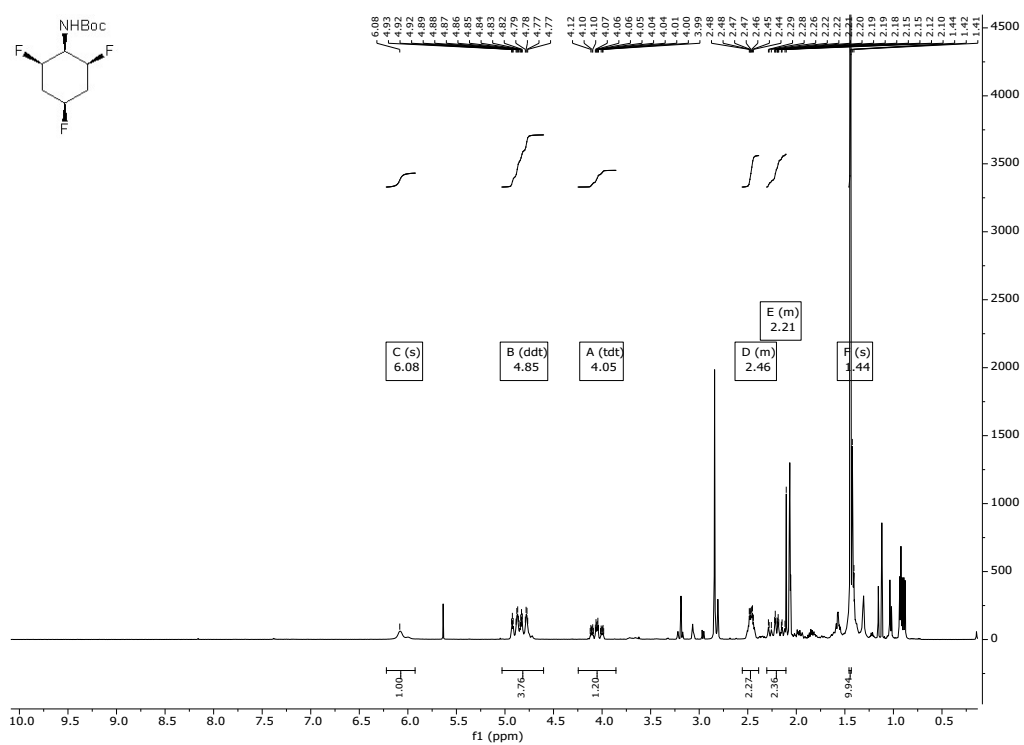
2D  $^1\text{H}$ -  $^{13}\text{C}$ -HSQC with multiplicity editing

$^{13}\text{C}$  NMR (176 MHz, Tol)  $^1\text{H}$  NMR (700 MHz, Tol)

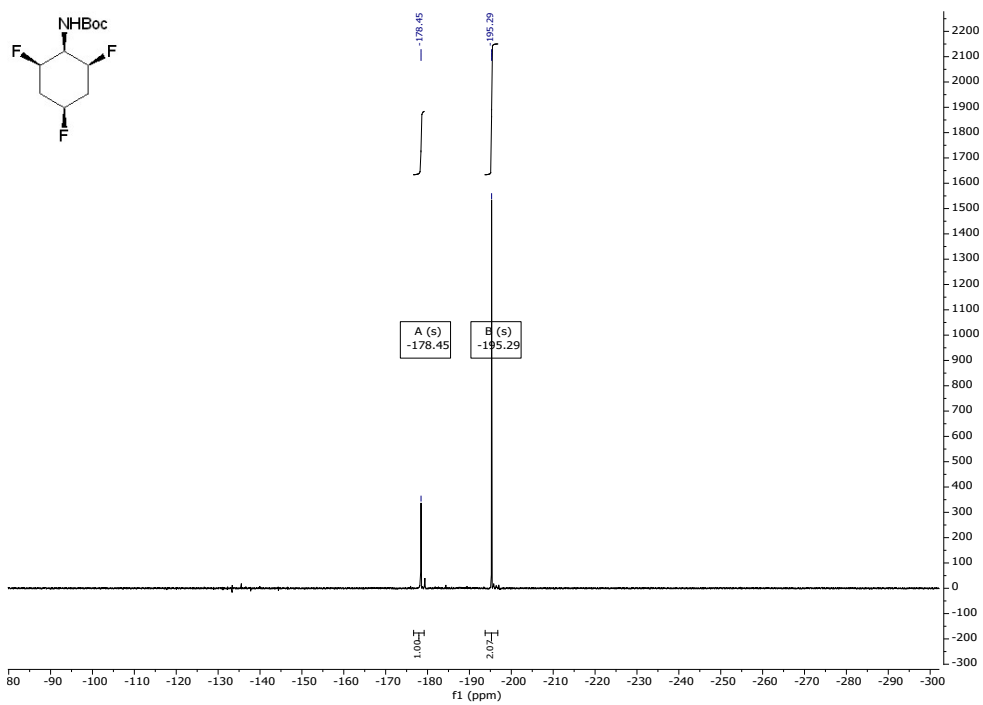


tert-butyl ((1*s*,2*R*,4*r*,6*S*)-2,4,6-trifluorocyclohexyl) carbamate (10)

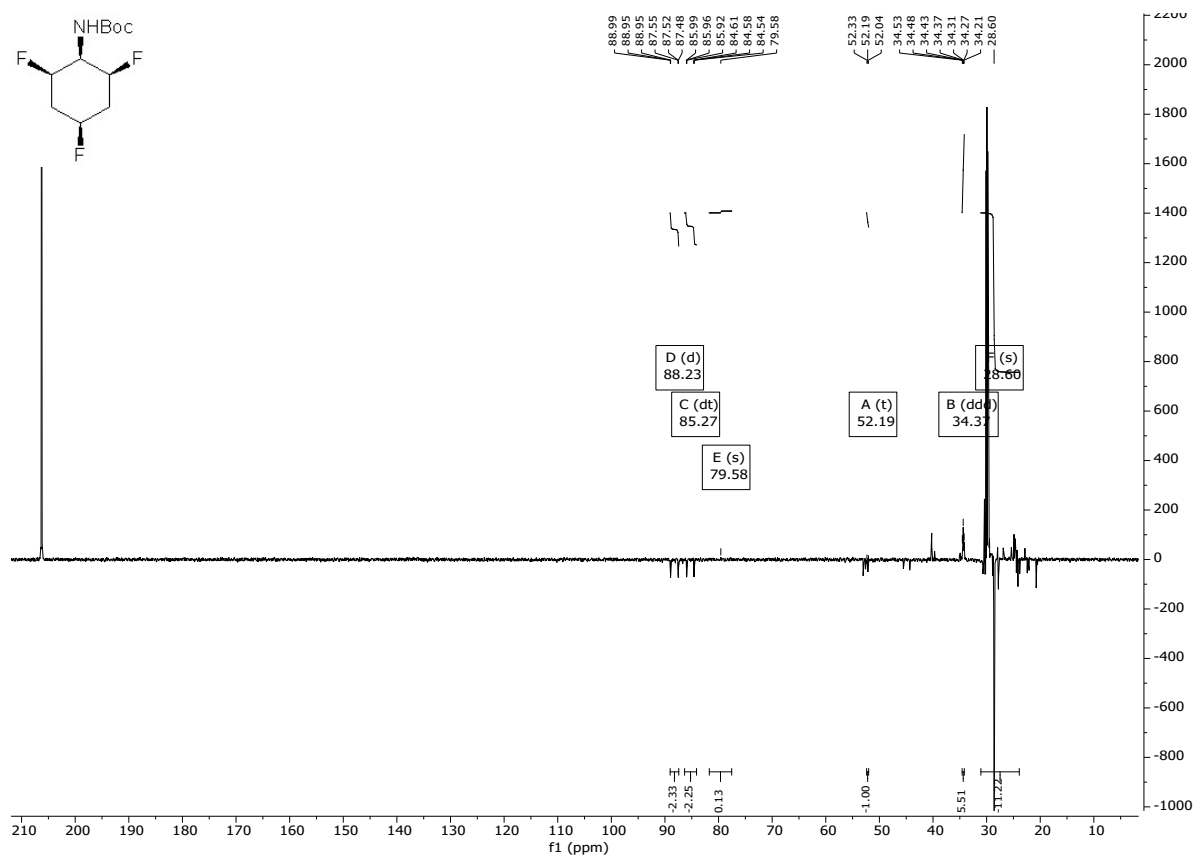
$^1\text{H}$  NMR (500 MHz, Acetone- $d_6$ )



<sup>19</sup>F NMR (470 MHz, Acetone-*d*<sub>6</sub>)

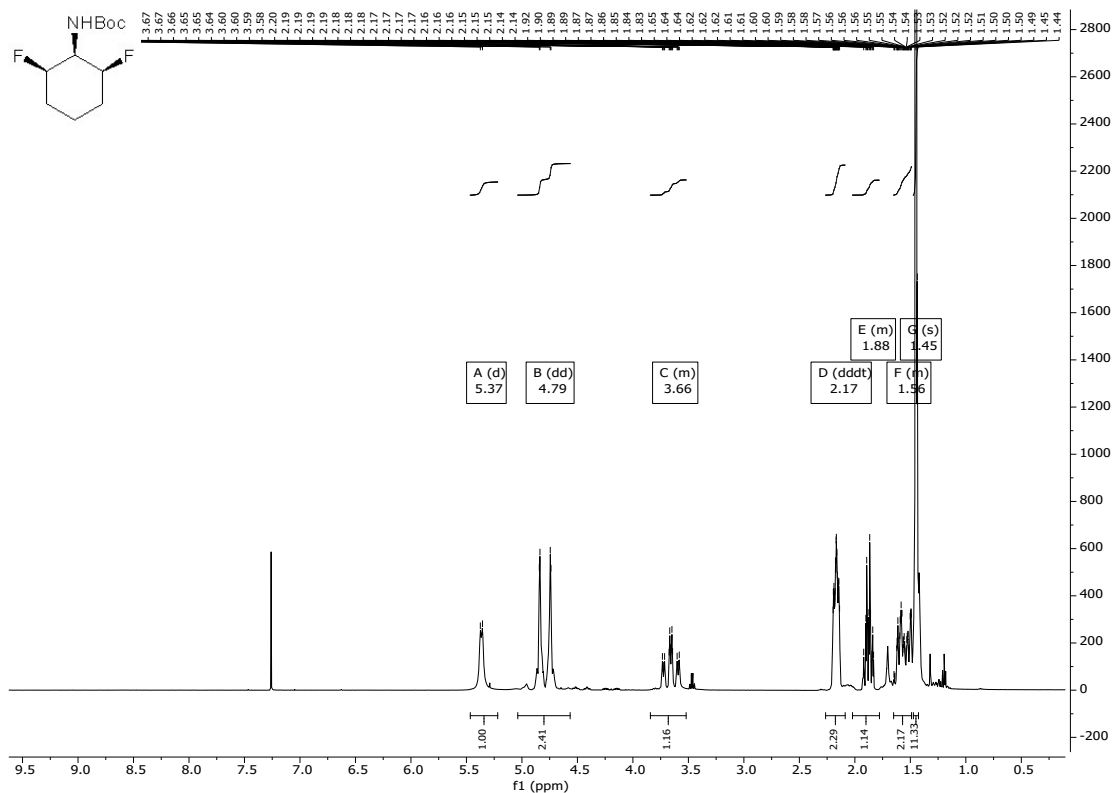


<sup>13</sup>C NMR (126 MHz, Acetone-*d*<sub>6</sub>)

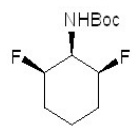


**tert-butyl ((1*s*,2*R*,6*S*)-2,6-difluorocyclohexyl) carbamate (12)**

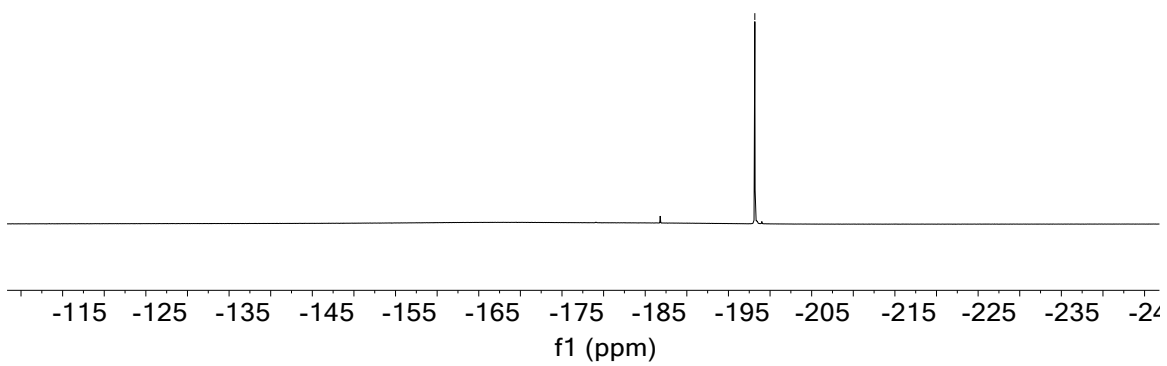
<sup>1</sup>H NMR (500 MHz, Chloroform-*d*)



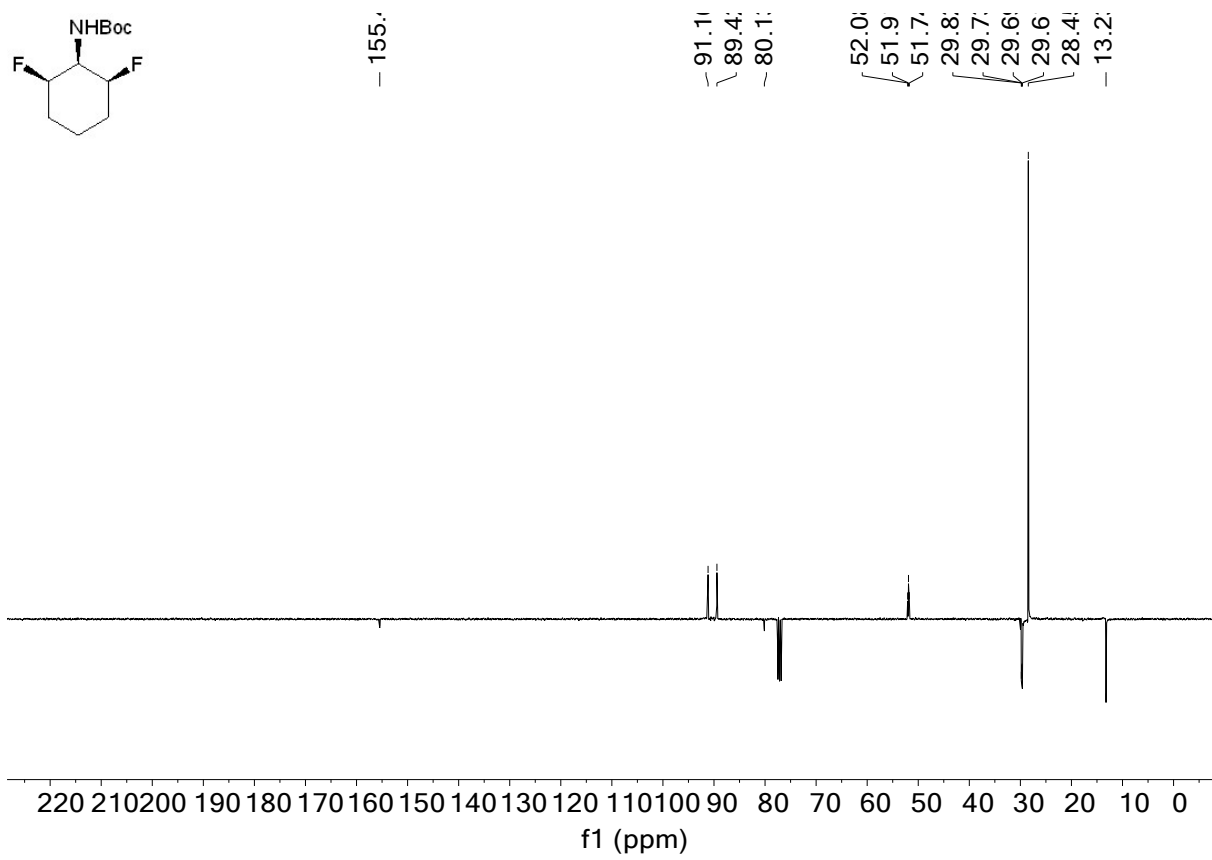
<sup>19</sup>F NMR (470 MHz, Chloroform-*d*)



-198



<sup>13</sup>C NMR (101 MHz, CDCl<sub>3</sub>)



### Reference

- M. P. Wiesenfeldt, Z. Nairoukh, W. Li, F. Glorius, *Science*, **2017**, *357*, 908-912.

## Details of X-ray diffraction data

X-ray diffraction data for compounds **5** and **10** were collected using a Rigaku MM-007HF High Brilliance RA generator/confocal optics with XtaLAB P100 diffractometer [Cu K $\alpha$  radiation ( $\lambda = 1.54187 \text{ \AA}$ )]. Diffraction data for compound **9** were collected using a Rigaku MM-007HF High Brilliance RA generator/confocal optics with XtaLAB P200 diffractometer [Cu K $\alpha$  radiation ( $\lambda = 1.54187 \text{ \AA}$ )]. Data for compounds **6**, **7** and **12** were collected using a Rigaku FR-X Ultrahigh Brilliance Microfocus RA generator/confocal optics with XtaLAB P200 diffractometer [Mo K $\alpha$  radiation ( $\lambda = 0.71073 \text{ \AA}$ )]. Intensity data were collected using either both  $\omega$  and  $\phi$  steps or just  $\omega$  steps accumulating area detector images spanning at least a hemisphere of reciprocal space. Data for all compounds analysed were collected using CrystalClear<sup>1</sup> and processed (including correction for Lorentz, polarization and absorption) using CrysAlisPro.<sup>2</sup> Structures were solved by dual space (SHELXT<sup>3</sup>) or direct methods (SIR2011<sup>4</sup>) and refined by full-matrix least-squares against F<sup>2</sup> (SHELXL-2018/3<sup>5</sup>). Non-hydrogen atoms were refined anisotropically, and hydrogen atoms were refined using a riding model. Compounds **6** and **10** showed pseudo-merohedric and non-merohedric twinning, respectively. Several of the crystals showed poorer than ideal data, for a variety of reasons, however, in all cases the structure was clear, particularly when considered in conjunction with other analytical data. Compound **6** appeared to give slightly polycrystalline crystals that diffracted weakly at high angles, the best data available is presented. Even this data shows signs that the twin law does not fully account for the polycrystallinity, resulting in the slightly elevated value of  $R_{\text{int}}$ . Compound **9** showed particularly weak diffraction with severe loss of data at higher angles, as well as signs of polycrystallinity or twinning that could not successfully be modelled, leading to elevated values of  $R_{\text{int}}$ ,  $R_I$  and  $wR_2$ . In addition the relative sizes of thermal ellipsoids for the three fluorine atoms suggests possible discrepancies in their occupancies such that they could refine to a total of only two fluorine atoms across the three sites. This can however be discounted on the basis of the chemical knowledge of the sample from other analytical techniques. All crystals of compound **12** showed some degree of polycrystallinity that reduced diffraction intensity at high angles, the best available data is presented. This could not be successfully modelled as twinning, leading to slightly elevated values of  $R_I$  and  $wR_2$ . All calculations were performed using either the Olex2<sup>6</sup> interface. Selected crystallographic data are presented in Table S1. CCDC 2202377-2202382 contains the supplementary crystallographic data for this paper. These data can be obtained free of charge from The Cambridge Crystallographic Data Centre via [www.ccdc.cam.ac.uk/structures](http://www.ccdc.cam.ac.uk/structures).

## References for Crystallography

1. *CrystalClear-SM Expert v2.1*. Rigaku Americas, *The Woodlands, Texas, USA*, and Rigaku Corporation, *Tokyo, Japan*, 2015.
2. *CrysAlisPro v1.171.39.8d, v1.171.40.14a, v1.171.41.93a, v1.171.42.38a*. Rigaku Oxford Diffraction, Rigaku Corporation, *Oxford, U.K.*, 2015-2021.
3. Sheldrick, G. M. SHELXT – Integrated space-group and crystal structure determination. *Acta Crystallogr., Sect. A: Found. Adv.* **2015**, *71*, 3-8. doi: 10.1107/S2053273314026370
4. Burla, M. C.; Caliandro, R.; Camalli, M.; Carrozzini, B.; Cascarano, G. L.; Giacovazzo, C.;

- Mallamo, M.; Mazzone, A.; Polidori, G.; Spagna, R. SIR2011: a new package for crystal structure determination and refinement. *J. Appl. Crystallogr.* **2012**, *45*, 357-361. doi: 10.1107/S0021889812001124
- 5. Sheldrick, G. M. Crystal structure refinement with SHELXL. *Acta Crystallogr., Sect. C: Struct. Chem.* **2015**, *71*, 3-8. Doi: 10.1107/S2053229614024218
  - 6. Dolomanov, O. V.; Bourhis, L. J.; Gildea, R. J.; Howard, J. A. K.; Puschmann, H. OLEX2: a complete structure solution, refinement and analysis program. *J. Appl. Crystallogr.* **2009**, *42*, 339-341. doi: 10.1107/S0021889808042726

Table S1. Selected crystallographic data.

	<b>5</b>	<b>6</b>	<b>7</b>	<b>9</b>	<b>10</b>	<b>12</b>
formula	C <sub>6</sub> H <sub>9</sub> F <sub>3</sub>	C <sub>7</sub> H <sub>11</sub> F <sub>3</sub>	C <sub>7</sub> H <sub>11</sub> OF <sub>3</sub>	C <sub>8</sub> H <sub>12</sub> F <sub>3</sub> NO	C <sub>11</sub> H <sub>18</sub> NO <sub>2</sub> F <sub>3</sub>	C <sub>11</sub> H <sub>19</sub> NO <sub>2</sub> F <sub>2</sub>
fw	138.13	152.16	168.16	195.18	253.26	235.27
temperature [K]	173	173	173	125	173	173
crystal description	Colourless needle	Colourless needle	Colourless plate	Colourless needle	Colourless plate	Colourless plate
crystal size [mm <sup>3</sup> ]	0.66×0.02×0.01	0.42×0.04×0.03	0.45×0.18×0.03	0.20×0.02×0.01	0.14×0.04×0.01	0.48×0.30×0.02
space group	<i>P</i> 1	<i>Cc</i>	<i>P</i> 2 <sub>1</sub> /c	<i>P</i> 2 <sub>1</sub>	<i>P</i> 1	<i>P</i> 2 <sub>1</sub> /c
<i>a</i> [Å]	4.7654(3)	4.8224(10)	12.7188(9)	9.161(2)	6.2763(4)	21.5717(6)
<i>b</i> [Å]	6.2994(4)	12.4436(19)	7.5388(5)	4.8349(8)	9.5541(4)	6.40500(10)
<i>c</i> [Å]	10.5867(6)	12.240(2)	8.2612(6)	9.983(3)	21.1552(10)	18.7016(4)
$\alpha$ [°]	89.429(5)				95.696(4)	
$\beta$ [°]	89.677(5)	90.55(2)	103.350(8)	105.30(3)	96.546(5)	106.865(3)
$\gamma$ [°]	73.640(6)				98.362(5)	
vol [Å <sup>3</sup> ]	304.92(3)	734.4(2)	770.72(10)	426.50(18)	1238.20(11)	2472.81(10)
<i>Z</i>	2	4	4	2	4	8
$\rho$ (calc) [g/cm <sup>3</sup> ]	1.504	1.376	1.449	1.520	1.359	1.264
$\mu$ [mm <sup>-1</sup> ]	1.338	0.132	0.142	1.267	1.058	0.105
F(000)	144.0	320.0	352.0	204.0	536.0	1008.0
reflections collected	3136	4594	16213	4826	25453	79325
independent reflections ( $R_{\text{int}}$ )	1079 (0.0314)	1567 (0.0948)	3673 (0.0485)	1619 (0.1421)	8795 (0.0659)	5643 (0.0845)
parameters, restraints	82, 0	93, 2	101, 0	119, 2	322, 2	295, 0
GoF on $F^2$	1.092	1.111	1.058	1.442	0.852	1.192
$R_I$ [ $I > 2\sigma(I)$ ]	0.0440	0.1075	0.0518	0.1848	0.0533	0.0911
$wR_2$ (all data)	0.1231	0.2933	0.1421	0.4428	0.1362	0.2053
largest diff. peak/hole [e/Å <sup>3</sup> ]	0.33, -0.21	0.74, -0.47	0.44, -0.21	1.36, -0.61	0.30, -0.26	0.50, -0.28

## Details of Computational Calculations

### - Geometry Optimization and Energy Calculations of Monomers

The B3LYP-D3/def2-TZVP theoretical level accurately reproduces the geometries and molecular assemblies of *Janus Face* compounds as demonstrated by the low RMSD calculated between theoretical and x-ray diffraction geometries (Fig S1). Therefore, geometric optimization and harmonic frequency calculations for compounds **1-7** and **9-12** were carried out at the B3LYP-D3/def2-TZVP theoretical level in order to identify each conformer as true energy minima, showing no imaginary frequencies using Gaussian 16 Rev C.01 program.<sup>1</sup> Single point energies were calculated over the monomeric optimized geometries using the Perdew-Burke-Ernzerhof hybrid functional (PBE0)<sup>2</sup> corrected with D3 empirical dispersion<sup>3</sup> and def2-TZVP basis set, since it was demonstrated in a previous publication that this theoretical level is a powerful method to compute highly accurate electronic energies of similar *Janus Face* compounds.<sup>4</sup> Thus, Gibbs free energy values shown throughout the text for compounds **1-7** and **9-12** are expressed in terms of the sum of PBE0-D3/def2-TZVP electronic energies and B3LYP-D3/def2-TZVP thermal correction to Gibbs free energy at standard pressure and temperature. Molecular dipole moments were also obtained at the PBE0-D3/def2-TZVP level.

NBO analysis was carried out at NBO 7.0 program as implemented in Gaussian 16 for compounds **9-12** over the B3LYP-D3/def2-TZVP optimized geometries using the PBE0-D3/def2-TZVP theoretical level using the LEWIS, NCE, STERIC and DIPOLE keywords.

### - Geometry Optimization and Complexation Energies of Trimers

The trimeric arrangements of compounds **5** and **6** were optimized at the B3LYP-D3/def2-TZVP theoretical level and harmonic frequency calculation was carried out at the same level in order to identify each structure as true energy minima, showing no imaginary frequencies using Gaussian 16 Rev C.01 program. The starting structures for the optimization of **5<sub>ax</sub>** and **6<sub>ax</sub>** trimers were extracted from the x-ray diffraction data and **5<sub>eq</sub>** trimer was manually constructed using **5<sub>ax</sub>** experimental structure as a model scaffold. It was noted that stacking **6<sub>eq</sub>** one molecule on top of another did not result in a local minimum, and direct geometry optimization always led to a less organized trimeric arrangement. Therefore, Grimme's iterative-static metadynamics (iMTD-sMTD) protocol implemented in CREST software<sup>5</sup> and GFN2-xTB method<sup>6</sup> was used to explore the conformational space of the **6<sub>eq</sub>** trimer, and the global minimum was re-optimized in DFT and used for further calculations. The same procedure was carried out for **7<sub>ax</sub>**, **9<sub>ax</sub>**, **10<sub>ax</sub>** and **12<sub>ax</sub>** trimers, and in each case the global minimum was in good agreement with the experimental structures, evincing the reliability of the methodology (Fig. S2).

A trimeric arrangement of **5<sub>ax</sub>** was also optimized using the molecular crystal QM/MM method as implemented in Ash software<sup>7</sup> in order to evaluate the influence of long-range interactions to trimer geometry. A spherical molecular cluster with radius of 35 Å was built and optimized at the GFN2-xTB level. However, the central trimer geometry obtained through this approach was in worse agreement to experiment if compared to the trimeric arrangement optimized in vacuo with B3LYP-D3/def2-TZVP, and therefore the latter methodology was adopted.

The BSSE-corrected complexation energies for the trimeric arrangement of compounds **5** and **6** were computed using the London Dispersion-corrected Hartree Fock method (HFLD)<sup>7</sup> and the aug-cc-pVTZ basis set as implemented in ORCA 5.0.3<sup>8</sup> due to its high accuracy – between that of DLPNO-CCSD and DLPNO-CCSD(T) schemes – and fast basis set convergence.

### - NMR Calculations

The general methodology used in computing NMR properties for compound **5** were extracted from Giovanetti *et al*<sup>9</sup> and is briefly described here. Structures of **5<sub>ax</sub>** and **5<sub>eq</sub>** were optimized considering implicit solvation (cyclohexane, toluene, chloroform and acetone) using the integral equation formalism to the polarized continuum model (IEF-PCM) in Gaussian 16 Rev C.01 program in B3LYP-D3/def2-TZVP and M06-L-D3/pc-1 theoretical levels. In both cases harmonic frequency calculations were carried out over the optimized structures in order to confirm each conformer as true energy minimum, showing no imaginary frequencies. Single point energies were computed for the optimized structures at the PBE0-D3/def2-TZVP theoretical level, and Boltzmann populations of **5<sub>ax</sub>** and **5<sub>eq</sub>** were estimated at 298.15K considering their relative Gibbs free energies expressed in terms of the sum of PBE0-D3/def2-TZVP electronic energies and B3LYP-D3/def2-TZVP (or M06-L-D3/pc-1) thermal correction to Gibbs free energy at standard pressure and temperature. The <sup>1</sup>J<sub>CF</sub> coupling constant was then calculated at the M06-L/pcJ-1 also in Gaussian 16 Rev C.01.

Solvation effect was also explicitly considered using the Quantum Cluster Growth<sup>10</sup> (QCG) workflow for xTB software.<sup>11</sup> Molecular clusters for each conformer of **5** were constructed with the addition of either 10 cyclohexane molecules, 10 toluene molecules, 20 chloroform molecules or 15 acetone molecules, always maintaining the solute fixed. The entire molecular cluster was then optimized in xTB using the GFN2-xTB semi-empirical method with “extreme” optimization thresholds. The optimized clusters were re-optimized using the QM1/QM2 method implemented in ORCA 5.0.3, where the solute was treated with a DFT method (both B3LYP-D3/def2-TZVP and M06-L-D3/pc-1) while solvent molecules were maintained fixed and were treated with GFN2-xTB method. Harmonic frequency calculations were carried out over the optimized structures in order to confirm each conformer as true energy minimum, showing no imaginary frequencies. Single point energies were computed for the optimized structures at the PBE0-D3/def2-TZVP theoretical level, and Boltzmann populations of **5<sub>ax</sub>** and **5<sub>eq</sub>** were estimated at 298.15K considering their relative Gibbs free energies expressed in terms of the sum of PBE0-D3/def2-TZVP electronic energies and B3LYP-D3/def2-TZVP (or M06-L-D3/pc-1) thermal correction to Gibbs free energy at standard pressure and temperature. The <sup>1</sup>J<sub>CF</sub> coupling constant was also calculated in the QM1/QM2 scheme, in which the solute was included in QM1 level and was treated with the M06-L/pcJ-1 theoretical level, and solvent molecules were included in QM2 level and treated with the GFN2-xTB method in ORCA 5.0.3.

All NMR results are shown in Table S1.

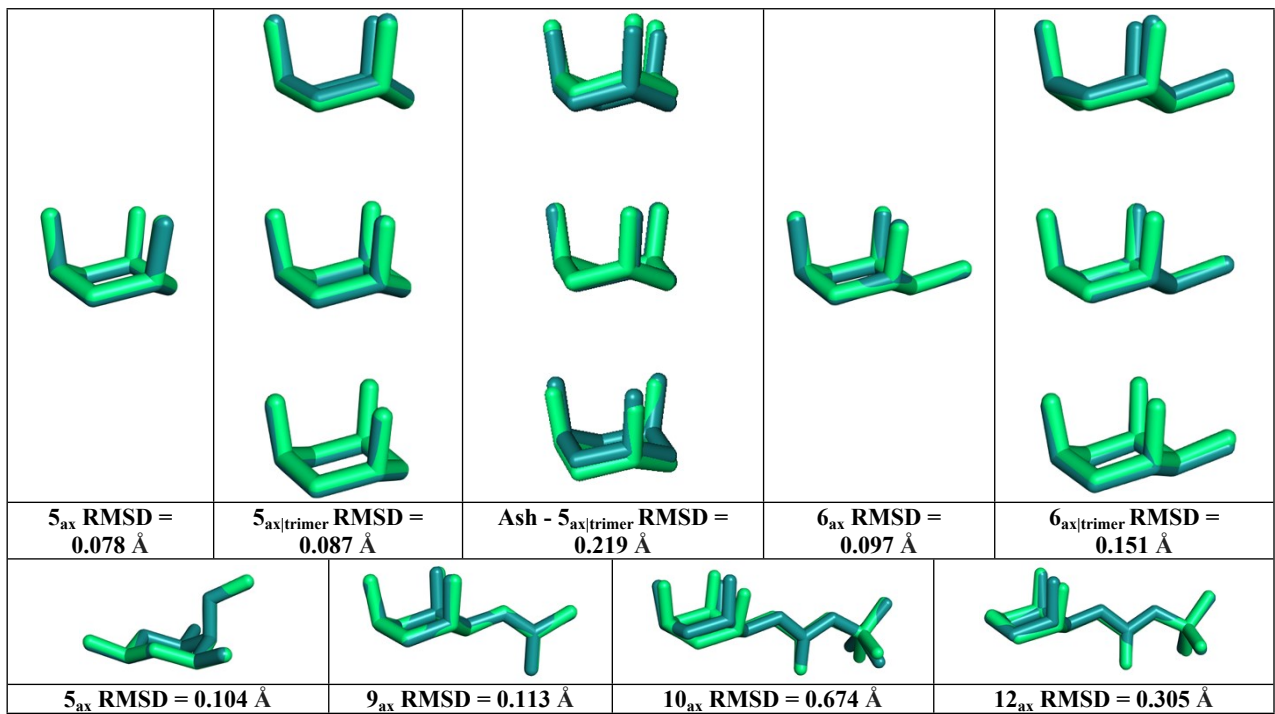


**Fig. S1** Superposition of X-ray diffraction (dark green) and calculated at B3LYP-D3/def2-TZVP theoretical level (light green) geometries with calculated RMSD over heavy atoms.

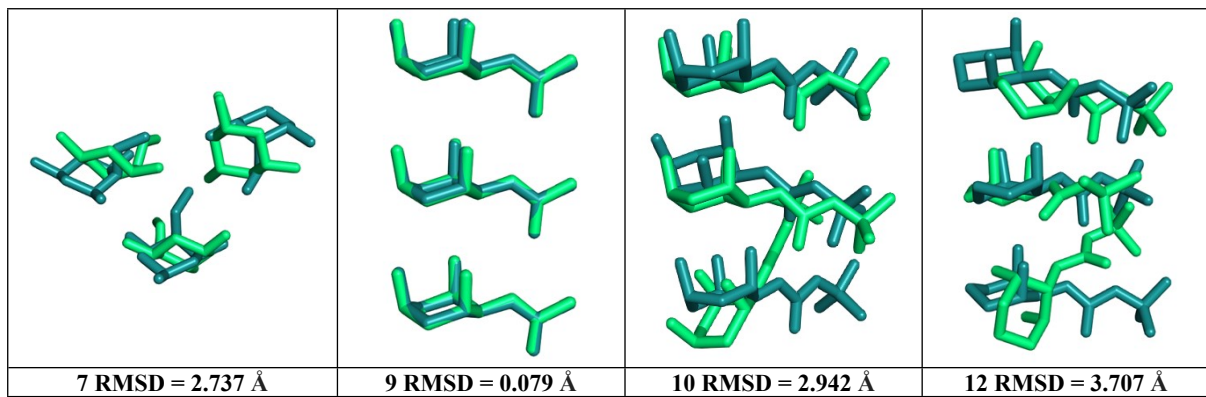


**Fig. S2** Superposition of X-ray diffraction (dark green) and calculated at GFN2-xTB//B3LYP-D3/def2-TZVP theoretical level (light green) trimer geometries with calculated RMSD over heavy atoms.

**Table S1** RMSD ( $\text{\AA}$ ) calculated over heavy atoms for the geometries obtained at B3LYP, B3LYP-D3, M06-2X, M06-2X-D3, M06L and M06L-D3 with the def2-TZVP basis set (B3LYP-D3/def2-TZVP geometry used as reference).

	<b>B3LYP</b>	<b>B3LYP-D3BJ</b>	<b>M06-2X</b>	<b>M06-2X-D3</b>	<b>M06L</b>	<b>M06L-D3</b>
<b>1</b>	0.008	0.004	0.017	0.017	0.012	0.011
<b>2ax</b>	0.013	0.007	0.100	0.098	0.016	0.052
<b>2eq</b>	0.013	0.010	0.015	0.015	0.013	0.013
<b>3ax</b>	0.008	0.004	0.014	0.014	0.013	0.013
<b>3eq</b>	0.007	0.004	0.013	0.013	0.011	0.011
<b>4ax</b>	0.007	0.003	0.011	0.011	0.016	0.016
<b>4eq</b>	0.007	0.004	0.014	0.014	0.012	0.012
<b>5ax</b>	0.013	0.005	0.017	0.017	0.019	0.020
<b>5eq</b>	0.005	0.003	0.015	0.015	0.015	0.015
<b>6ax</b>	0.006	0.008	0.015	0.015	0.018	0.018
<b>6eq</b>	0.011	0.006	0.014	0.014	0.016	0.016
<b>7ax</b>	0.029	0.008	0.099	0.099	0.094	0.095
<b>7eq</b>	0.037	0.015	0.038	0.038	0.064	0.062
<b>9ax</b>	0.137	0.137	0.127	0.127	0.061	0.061
<b>9eq</b>	0.013	0.005	0.028	0.029	0.019	0.019
<b>10ax</b>	0.364	0.067	0.063	0.069	0.040	0.047
<b>10eq</b>	0.017	0.009	0.030	0.030	0.032	0.074
<b>11ax</b>	0.013	0.012	0.304	0.305	0.014	0.224
<b>11eq</b>	0.015	0.006	0.092	0.120	0.019	0.029
<b>12ax</b>	0.287	0.041	0.058	0.064	0.025	0.030
<b>12eq</b>	0.013	0.007	0.023	0.023	0.086	0.090
<b>Average</b>	0.049	0.017	0.053	0.055	0.029	0.044

**Table S2** NBO analysis relative energies (in kcal mol<sup>-1</sup>) obtained at the PBE0-D3/def2-TZVP theoretical level for compounds **9–12**, where  $\Delta E(T)$  is the electronic,  $\Delta E(L)$  the Lewis,  $\Delta E(NL)$  the non-Lewis,  $\Delta E(NCE)$  the electrostatic and  $\Delta E(NSA)$  the steric energies. Positive values represent a preference for the equatorial conformer whereas negative ones for the axial conformer.

	$\Delta E(T)$	$\Delta E(L)$	$\Delta E(NL)$	$\Delta E(NCE)$	$\Delta E(NSA)$
<b>9</b>	-2.21	4.81	-7.03	0.32	-0.98
<b>10</b>	-1.34	4.86	-6.20	5.37	-2.19
<b>11</b>	-4.31	-3.50	-0.82	-7.56	0.35
<b>12</b>	-3.45	-3.56	0.11	-2.65	-1.28

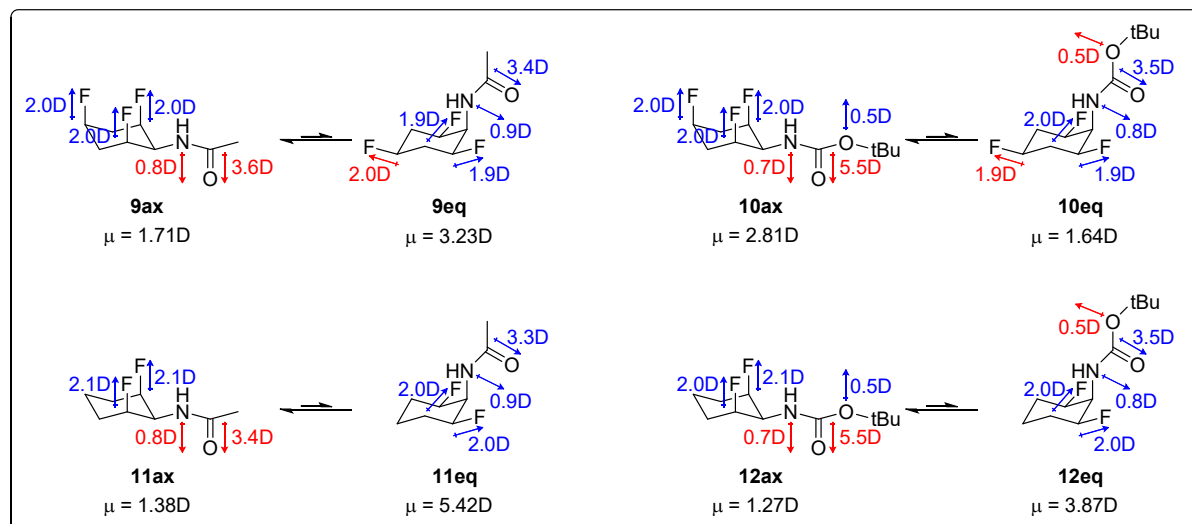
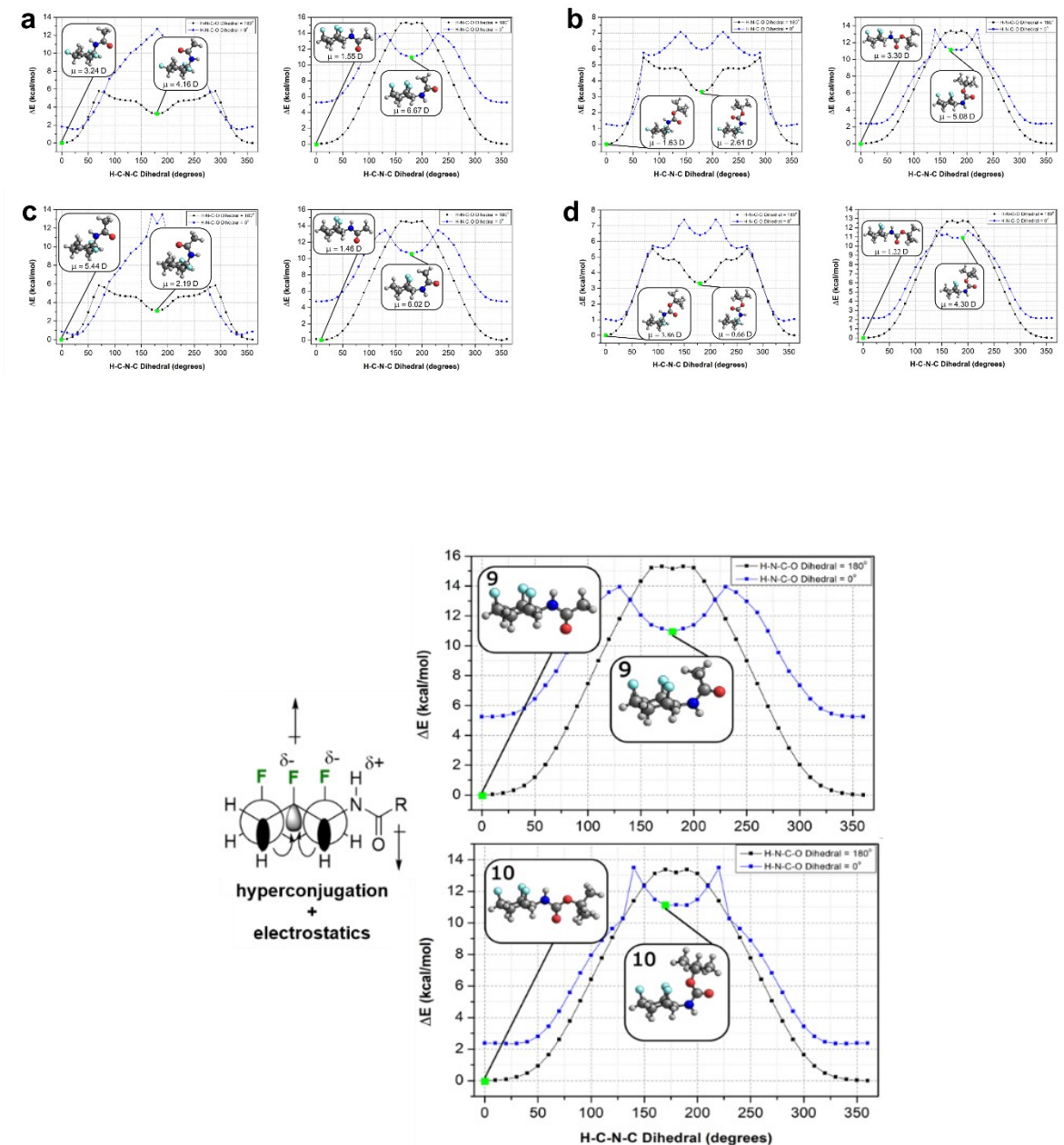


**Fig S3** Calculated contribution from the polar groups to molecular dipole moment in compounds **9–12** obtained from the NBO analysis. Dipole vectors/dipole values in blue and red represent dipoles in opposite directions.

NBO analysis suggest that electrostatic effects are the most important in stabilizing the axial C-F conformers, mostly due to  $F_{\text{ax}}\text{-}F_{\text{ax}}$  electrostatic repulsion minimization in **9<sub>ax</sub>** and **10<sub>ax</sub>** (each accounting for  $\sim 15.8$  kcal mol<sup>-1</sup> in destabilizing energy) and due to  $F_{\text{ax}}\text{-H}_{\text{ax}}$  stabilizing electrostatic interactions in **11<sub>ax</sub>** and **12<sub>ax</sub>** (each accounting for  $\sim 10.5$  kcal mol<sup>-1</sup> in stabilizing energy). For instance, the [ $\Delta E(\text{NCE})$ ] energy assumes positive values for both **9** and **10**, representing overall electrostatic stabilization of the equatorial conformers; and negative values in **11** and **12**, indicating overall axial stabilization. On the other hand, hyperconjugative energy [ $\Delta E(\text{NL})$ ] is in **9**, **10** and **11** axial-stabilizing and equally stabilizing axial and equatorial in **12**. This is mainly due to  $\sigma_{\text{CH}} \rightarrow \sigma^*_{\text{CF}}$  hyperconjugative interactions ( $\sim 5.2$  kcal mol<sup>-1</sup> each) that are present in axial conformers and are replaced by  $\sigma_{\text{CH}} \rightarrow \sigma^*_{\text{CH}}$  ( $\sim 2.6$  kcal mol<sup>-1</sup> each) in the equatorial counterparts. Finally, steric effects are in general of smaller importance than hyperconjugation and electrostatics since the bulky substituents (NHAc and NHBoc) are in all cases pointing on the opposite direction of the cyclohexane ring.

In addition, the decomposition of the molecular dipole moment into each NLMO contribution in compounds **9–12** show that besides electrostatic stabilization, the removal of a fluorine atom heavily increases equatorial conformers dipole moment (main dipole vectors are illustrated in Fig S3) which leads to overall molecular destabilization and favour the axial conformers. Note that the molecular dipole moment does not change much going from **9<sub>ax</sub>** to **11<sub>ax</sub>**, even though there are three parallel C-F<sub>ax</sub> bonds in the former and only two in

the latter. This can be rationalized by the amide orientation with respect to the C-F<sub>ax</sub> bonds: the H-C-N-C dihedral angle is 0° in the global minimum geometry of **9<sub>ax</sub>** and therefore its dipole is perfectly anti-parallel to the C-F<sub>ax</sub> bonds, being more effective in molecular dipole moment minimization. Conversely, in **11<sub>ax</sub>** the H-C-N-C dihedral angle is of 10°, and in this case the amide dipole is slightly tilted with respect to the C-F<sub>ax</sub> bonds, resulting in a less effective molecular dipole moment minimization. However, in both NHBoc-substituted cyclohexanes **10<sub>ax</sub>** and **12<sub>ax</sub>** the adopted H-C-N-C dihedral angle in the global minima geometries is of 0°. In those cases, the NHBoc dipole moment is contributing to molecular dipole moment minimization equally to **10<sub>ax</sub>** and **12<sub>ax</sub>**, and the removal of a C-F<sub>ax</sub> results in a molecular dipole moment roughly 1.5 D lower. The relaxed energy profile (PES) around H-C-N-C dihedral angles for compounds **9-12** are illustrated in Fig S4.



Rotational energy profiles for triaxial **9<sub>ax</sub>** and **10<sub>ax</sub>**. H-N-C-O dihedral angles of 180° are favoured with deep energy wells for conformers with N-H *syn* and C=O *anti* to the axial C-F bonds.<sup>20c</sup>

**Fig. S4** Relaxed energy profile (PES) of compounds **9** (a), **10** (b), **11** (c) and **12** (d) rotating around the C-NHAc (or C-NHBoc) in steps of 10° for the triaxial and triequatorial conformers obtained at the B3LYP-D3/def2-TZVP theoretical level.

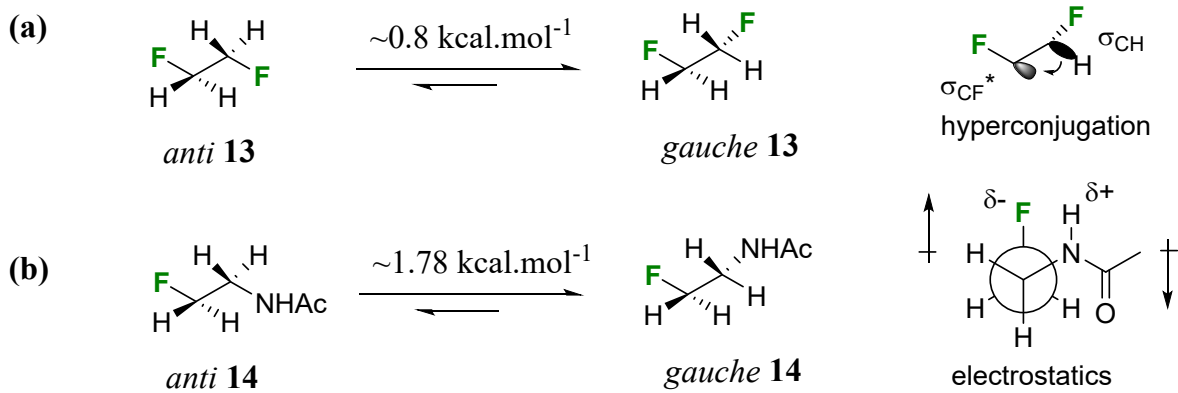


**Fig. S5** (a) Fluorine *gauche* effect<sup>16</sup>; (b) Fluorine-amide *gauche*.<sup>16c</sup>

**Table S3** Calculated  $\Delta G$ , conformer population and  $^1J_{\text{CF}}$  obtained from the implicit and explicit solvation models tested.

Solvent	Implicit Solvation			M06-L-D3/pc-1 Geometry			Experimental $^1J_{\text{CF}}$
	B3LYP-D3/def2-TZVP Geometry	$\Delta G$ (kcal mol <sup>-1</sup> )	Pop <sup>[a]</sup> (%) (ax/eq)	$^1J_{\text{CF}}$	$\Delta G$ (kcal mol <sup>-1</sup> )	Pop <sup>[a]</sup> (%) (ax/eq)	
Cyclohexane		2.95	0.8/99.2	161.2 Hz	3.03	0.6/99.4	157.6 Hz
Toluene		2.73	1.2/98.8	160.3 Hz	2.82	0.9/99.1	157.2 Hz
Chloroform		2.01	5.0/95.0	158.2 Hz	2.31	2.0/98.0	156.1 Hz
Acetone		1.15	12.7/87.3	156.2 Hz	1.47	7.7/92.3	154.8 Hz
MAE				17.5 Hz			20.0 Hz
Explicit Solvation							
Solvent	B3LYP-D3/def2-TZVP Geometry	$\Delta G$ (kcal mol <sup>-1</sup> )	Pop (%) (ax/eq)	$^1J_{\text{CF}}$	M06-L-D3/pc-1 Geometry	Pop (%) (ax/eq)	Experimental $^1J_{\text{CF}}$
Cyclohexane		3.12	0.5/99.5	184.2 Hz	3.43	0.3/99.7	178.9 Hz
Toluene		1.22	11.4/88.6	179.7 Hz	1.88	4.0/96.0	177.4 Hz
Chloroform		1.00	15.5/84.5	174.0 Hz	0.95	16.8/83.2	172.4 Hz
Acetone		0.06	47.3/52.7	173.2 Hz	-0.03	51.3/48.7	170.8 Hz
MAE				2.5 Hz			1.8 Hz

<sup>[a]</sup> Boltzmann population obtained from calculated  $\Delta G$ ,  $k_b = 0.001987 \text{ kcal}/(\text{mol K})$  and  $T = 298.15 \text{ K}$ .

**Table S4** Cartesian coordinates and Lowest harmonic vibrational frequencies of the optimized geometries for monomers, trimers and explicit solvation clusters studied calculated at the B3LYP-D3/def2-TZVP level in the gas-phase. Electronic energies were calculated over the optimized geometries at PBE0-D3/def2-TZVP theoretical level.

1 Energy (hartrees) = -830.802495 Lowest harmonic vibrational frequency (cm <sup>-1</sup> ) = 108.53						
F	0.0000000	1.6201900	1.14377700			
F	-2.38046500	1.37436200	-0.26293300			
F	-1.40312600	-0.81009500	1.14377700			
F	0.00000000	-2.74872500	-0.26293300			
F	1.40312600	-0.81009500	1.14377700			
F	2.38046500	1.37436200	-0.26293300			
C	0.0000000	1.47625000	-0.22511500			
C	-1.24389400	0.71816300	-0.68864500			
C	-1.27847000	-0.73812500	-0.22511500			
C	0.00000000	-1.43632600	-0.68864500			
C	1.27847000	-0.73812500	-0.22511500			
C	1.24389400	0.71816300	-0.68864500			
H	0.00000000	2.48000300	-0.65917800			
H	-1.25134200	0.72246200	-1.78586000			
H	-2.14774600	-1.24000200	-0.65917800			
H	0.00000000	-1.44492500	-1.78586000			
H	2.14774600	-1.24000200	-0.65917800			
H	1.25134200	0.72246200	-1.78586000			
2 <sub>ax</sub> Energy (hartrees) = -651.095750 Lowest harmonic vibrational frequency (cm <sup>-1</sup> ) = 93.51				2 <sub>eq</sub> Energy (hartrees) = -651.085226 Lowest harmonic vibrational frequency (cm <sup>-1</sup> ) = 98.74		
C	-1.41584700	0.42071700	-0.69603600	C	0.24189200	1.40882400
C	-1.06689700	-1.01075400	-0.28895800	C	-1.16064600	0.96478500
C	0.34362600	-1.43639900	-0.69599200	C	-1.34081400	-0.49494500
C	1.40883600	-0.41833500	-0.28911700	C	-0.25526800	-1.48742600
C	1.07199600	1.01609100	-0.69598200	C	1.09928000	-0.91384700
C	-0.34207400	1.42938100	-0.28844700	C	1.41592900	0.52259800
H	-1.79029100	-1.69622500	-0.74507300	H	-1.86066000	1.54718100
H	-1.42016800	0.42227100	-1.79347000	H	0.24870900	1.44906900
H	2.36400200	-0.70203000	-0.74566500	H	-0.40945600	-2.38521000
H	1.07533900	1.01965700	-1.79342000	H	1.13077300	-0.93998200
H	-0.57409600	2.39884700	-0.74396800	H	2.27027900	0.83789500
H	0.34469100	-1.44139000	-1.79342600	H	-1.37876400	-0.50906100
F	-0.39232200	1.63802300	1.09542000	C	1.85391800	0.68404200
F	-1.22343500	-1.15907700	1.09474100	H	2.72952900	0.06296600
F	1.61604000	-0.47994800	1.09445200	H	2.12069100	1.72405200
C	0.67999600	-2.84083700	-0.19760800	H	1.09166300	0.40531100
H	-0.05533500	-3.56496600	-0.55360100	C	-1.52029800	1.26279300
H	1.66393400	-3.15283600	-0.55305800	H	-1.42163200	2.33173100
H	0.68512300	-2.86345300	0.89027600	H	-2.55423300	0.97283800
C	-2.80053500	0.83173100	-0.19833800	H	-0.89796200	0.74270400
H	-3.05960100	1.83069400	-0.55437200	C	-0.33443700	-1.94680200
H	-3.56260400	0.13578800	-0.55434800	H	-1.30980900	-2.39523600
H	-2.82335500	0.83853000	0.88954400	H	0.43320800	-2.69739700
C	2.12053400	2.00951100	-0.19818300	H	-0.19537600	-1.14707700
H	3.11512800	1.73430200	-0.55433300	F	-2.59247500	-0.95713200
H	1.89904200	3.01757700	-0.55395900	F	0.46782200	2.72376700
H	2.13784400	2.02561400	0.88968000	F	2.12528600	-1.76662600
3 <sub>ax</sub> Energy (hartrees) = -731.620767 Lowest harmonic vibrational frequency (cm <sup>-1</sup> ) = 106.79				3 <sub>eq</sub> Energy (hartrees) = -731.624973 Lowest harmonic vibrational frequency (cm <sup>-1</sup> ) = 99.82		
C	-1.28210600	0.95394200	-0.36219900	C	1.24038400	-0.93230600
C	0.00000100	1.63913200	-0.83292800	C	1.27511400	0.56813900
C	1.28210900	0.95393400	-0.36221100	C	0.000005100	1.20775600
C	1.23898400	-0.54037800	-0.66082700	C	-1.27505000	0.56825900
C	-0.00000500	-1.23908300	-0.10977900	C	-1.24050600	-0.93219000
C	-1.23898900	-0.54036800	-0.66082600	C	-0.000007900	-1.58399800
H	2.15130000	1.38657800	-0.86599200	H	2.15132900	1.02679800
H	-0.00000400	1.67738200	-1.92631100	H	-2.15123700	1.02702800
H	0.00000800	2.66780800	-0.47238800	H	-1.27506200	-1.08422700
H	-2.15130200	1.38658900	-0.86597000	H	-0.000009500	-1.44483000
H	1.23154500	-0.65630800	-1.75209300	H	-0.000014100	-2.65157000
H	-0.00001300	-2.28818800	-0.41930700	H	0.000003700	1.08389000
H	-1.23154200	-0.65628600	-1.75209300	F	2.38335100	-1.51806900
F	-1.45994800	1.16592500	0.99577600	H	1.27494700	-1.08433500
F	-0.00000400	-1.21929500	1.26864200	F	0.00011400	2.56460400
F	-2.38036900	-1.16075100	-0.18638400	F	1.37533300	0.77746100
F	1.45996700	1.16592400	0.99576000	F	-1.37520100	0.77751700
F	2.38036000	-1.16076400	-0.18637500	F	-2.38351300	-1.51781500
4 <sub>ax</sub> Energy (hartrees) = -632.436694				4 <sub>eq</sub> Energy (hartrees) = -632.443432		







<p style="text-align: center;"><b><math>5_{\text{ax toluene}}</math></b>  <b>Energy (hartrees) = -533.224439</b>  <b>Lowest harmonic vibrational frequency (cm<sup>-1</sup>) = 111.66</b></p>	<p style="text-align: center;"><b><math>5_{\text{eq toluene}}</math></b>  <b>Energy (hartrees) = -533.227175</b>  <b>Lowest harmonic vibrational frequency (cm<sup>-1</sup>) = 164.62</b></p>











C 0.442037000 1.274212000 -0.300195000 C -0.101691000 1.268369000 -0.755720000 C -1.773601000 0.000000000 -0.399337000 H 0.957677000 -2.135677000 -0.737916000 H -1.026507000 -1.380957000 -1.844577000 H 0.957676000 2.135676000 -0.737920000 H -1.026509000 1.380958000 -1.844576000 H -2.741550000 0.000000000 -0.910080000 H 1.251096000 -0.000001000 -1.772469000 F -2.059799000 0.000000000 0.969747000 F 0.488473000 -1.463680000 1.085423000 F 0.488476000 1.463682000 1.085421000 C 2.623158000 -0.000001000 -0.117385000 H 3.170463000 -0.884027000 -0.450216000 H 3.170455000 0.884041000 -0.450186000 H 2.600119000 -0.000018000 0.970571000 H -1.525387000 2.131525000 -0.331178000 H -1.525387000 -2.131526000 -0.331180000	C -0.904787000 -1.262591000 0.091625000 C 0.460217000 -1.235121000 -0.581557000 C 1.291764000 0.000003000 -0.216392000 H -1.458110000 2.145260000 -0.230393000 H 0.336188000 1.279369000 -1.669525000 H -1.458084000 -2.145283000 -0.230297000 H 0.336161000 -1.279358000 -1.669511000 H 2.176158000 -0.000001000 -0.859599000 H -1.955289000 -0.000042000 -1.311715000 C 1.766036000 0.000012000 1.238201000 H 2.370917000 -0.885139000 1.429583000 H 2.371166000 0.885012000 1.429491000 H 0.940781000 0.000176000 1.950252000 F -2.886027000 -0.000007000 0.462651000 F 1.164182000 2.392200000 -0.227634000 F 1.164202000 -2.392196000 -0.227657000 H -0.781767000 -1.322556000 1.174225000 H -0.781817000 1.322600000 1.174177000
<b>6<sub>ax</sub> trimer</b> <b>Energy (hartrees) = -1719.508526</b> <b>Lowest harmonic vibrational frequency (cm<sup>-1</sup>) = 17.99</b>	<b>6<sub>eq</sub> trimer</b> <b>Energy (hartrees) = -1719.508664</b> <b>Lowest harmonic vibrational frequency (cm<sup>-1</sup>) = 8.53</b>
F -5.851436000 -1.944218000 -0.000365000 F -5.760281000 0.635233000 -1.477396000 F -5.760863000 0.633807000 1.476955000 C -4.045803000 -1.018677000 1.266214000 H -2.962376000 -1.113932000 1.365443000 C -4.459212000 -1.750333000 -0.000512000 H -4.018506000 -2.751520000 -0.000803000 C -4.046181000 -1.018115000 -1.267059000 H -2.962949000 -1.114336000 -1.367464000 C -4.379510000 0.465161000 -1.273476000 H -3.892154000 0.941111000 -2.130369000 C -3.944135000 1.186154000 0.000339000 H -2.852701000 1.128544000 0.000709000 C -4.379985000 0.464384000 1.273553000 H -3.893178000 0.940024000 2.130939000 C -4.367552000 2.653013000 0.000671000 H -3.982018000 3.165994000 -0.883341000 H -5.452837000 2.738235000 0.000570000 H -3.982203000 3.165513000 0.885042000 F -1.090332000 -2.047775000 0.000055000 F -1.061676000 0.494354000 -1.483225000 F -1.061775000 0.493382000 1.483767000 C 0.703590000 -1.100461000 1.266132000 H 1.789459000 -1.166650000 1.360194000 C 0.304713000 -1.839116000 0.000012000 H 0.751795000 -2.836266000 -0.000159000 C 0.703284000 -1.100105000 -1.266003000 H 1.789079000 -1.166566000 -1.360806000 C 0.328060000 0.372328000 -1.274006000 H 0.796503000 0.864193000 -2.130985000 C 0.729681000 1.110608000 0.000490000 H 1.822627000 1.097093000 0.000620000 C 0.328010000 0.371850000 1.274687000 H 0.796209000 0.863565000 2.131888000 C 0.249303000 2.560271000 0.000742000 H 0.614030000 3.087488000 -0.883139000 H -0.838036000 2.609257000 0.000836000 H 0.614189000 3.087218000 0.884720000 F 3.695264000 -2.015527000 0.000329000 F 3.641491000 0.502727000 -1.468642000 F 3.642204000 0.502226000 1.468682000 C 5.458230000 -1.025904000 1.267510000 H 6.546602000 -1.065041000 1.374696000 C 5.081459000 -1.777165000 -0.000225000 H 5.551630000 -2.763822000 -0.000418000 C 5.457284000 -1.025913000 -1.268245000 H 6.545570000 -1.065204000 -1.376279000 C 5.033110000 0.435108000 -1.274755000 H 5.474255000 0.943546000 -2.136844000 C 5.412671000 1.190476000 -0.000324000 H 6.509635000 1.227206000 -0.000578000 C 5.033775000 0.435033000 1.274251000 H 5.475125000 0.943584000 2.136168000 C 4.874814000 2.620363000 -0.000137000 H 5.215869000 3.162291000 -0.883763000 H 3.786679000 2.620530000 0.000280000 H 5.216560000 3.162307000 0.883212000 H -4.509560000 -1.498549000 2.129882000 H -4.511080000 -1.497099000 -2.130617000 H 0.259288000 -1.593386000 2.132390000 H 0.258381000 -1.592611000 -2.132196000 H 5.029379000 -1.532198000 2.133308000 H 5.027716000 -1.532160000 -2.133717000	
7 <sub>ax</sub>	7 <sub>eq</sub>





- Scalmani, V. Barone, G. A. Petersson, H. Nakatsuji, X. Li, M. Caricato, A. V. Marenich, J. Bloino, B. G. Janesko, R. Gomperts, B. Mennucci, H. P. Hratchian, J. V. Ortiz, A. F. Izmaylov, J. L. Sonnenberg, D. Williams-Young, F. Ding, F. Lipparini, F. Egidi, J. Goings, B. Peng, A. Petrone, T. Henderson, D. Ranasinghe, V. G. Zakrzewski, J. Gao, N. Rega, G. Zheng, W. Liang, M. Hada, M. Ehara, K. Toyota, R. Fukuda, J. Hasegawa, M. Ishida, T. Nakajima, Y. Honda, O. Kitao, H. Nakai, T. Vreven, K. Throssell, J. A. Montgomery, Jr., J. E. Peralta, F. Ogliaro, M. J. Bearpark, J. J. Heyd, E. N. Brothers, K. N. Kudin, V. N. Staroverov, T. A. Keith, R. Kobayashi, J. Normand, K. Raghavachari, A. P. Rendell, J. C. Burant, S. S. Iyengar, J. Tomasi, M. Cossi, J. M. Millam, M. Klene, C. Adamo, R. Cammi, J. W. Ochterski, R. L. Martin, K. Morokuma, O. Farkas, J. B. Foresman, and D. J. Fox, Gaussian, Inc., Wallingford CT, 2016.
2. J. Perdew, M. Ernzerhof, K. Burke, *J. Chem. Phys.*, **1996**, 105, 9982.
  3. S. Grimme, J. Antony, S. Ehrlich, H. Krieg, *J. Chem. Phys.*, **2010**, 132, 154104.
  4. T. J. Poskin, B. A. Piscelli, K. Yoshida, D. B. Cordes, A. M. Z. Slawin, R. A. Cormannich, S. Yamada, D. O'Hagan, *Chem. Commun.*, **2022**, 58, 7968-7971.
  5. P. Pracht, F. Bohle, S. Grimme, *PhysChemChemPhys*, **2020**, 22, 7169-7192.
  6. C. Bannwarth, S. Ehlert, S. Grimme, *J. Chem. Theory Comput.*, **2019**, 15, 1652-1671.
  7. A. Altun, F. Neese, G. Bistoni, *J. Chem. Theory Comput.*, **2019**, 15, 11, 5894-5907.
  8. F. Neese, F. Wennmohs, U. Becker, C. Ripplinger, *J. Chem. Phys.*, **2020**, 152, 224108.
  9. M. Giovanetti, L. F. F. Bitencourt, R. A. Cormannich, S. P. A. Sauer, *J. Chem. Theory Comput.*, **2021**, 17, 12, 7712-7723.
  10. S. Spicher, C. Plett, P. Pracht, A. Hansen, S. Grimme, *J. Chem. Theory Comput.*, **2022**, 18, 5, 3174-3189.
  11. C. Bannwarth, E. Caldeweyher, S. Ehlert, A. Hansen, P. Pracht, J. Seibert, S. Spicher, S. Grimme, *WIREs Comput. Mol. Sci.*, **2021**, 11, 1493-1542.